Evaluation of improvements in Near-Real Time Ocean Color Data Processing at NOAA CoastWatch

Sathyadev Ramachandran[1,2], Menghua Wang[1]

[1]NOAA/NESDIS/STAR/SOCD, 5200 Auth Rd, Camp Springs, MD 20746, USA

[2]SP Systems Inc, 7500 Greenway Center Dr., Suite 850, Greenbelt, MD 20770, USA

ABSTRACT

We investigate improvements to the quality of our NOAA CoastWatch near-real-time Ocean Color products that can be made with the appropriate choice of the Ancillary data sources which are used in the processing of the L1B calibrated radiances to L2 Ocean Color products like the normalized water leaving radiances, nLw in the bands 412, 443, 488, 531, 551 and 667 nm as well as the bio-optical products further derived from these radiances using empirical algorithms like for the Chlorophyll concentration for the MODIS Aqua sensor. In our study we limited the regions to four representative areas around the CONUS and for four seasons of a calendar year. Our recommended choice for the best Ancillary data source, the NCEP GFS model forecast was selected based on the results from this study will be used to process L1B data from different sensors and for all regions of interest at NOAA CoastWatch in the future.

Introduction

Ocean color measurements from satellite platforms face the challenge of accurately accounting for the contribution of the various constituents in the atmosphere to the total radiances measured by the sensor at the satellite altitude to estimate the water leaving radiances at the interface of the ocean surface and the atmosphere. The water leaving radiances are proxies to the bio-optical state of the ocean and appropriate ratios of these radiances can be used in empirical algorithms to derive the chlorophyll concentration and various other useful products for monitoring the oceans. The correction methods and data

used to accomplish this has significant implications on the end products estimated, as less than 10% of the measured radiance at the top of the atmosphere constitute the contribution from the water column just below the ocean surface. The rest 90 % of the signal being from the atmospheric scattering processes involving molecular constituents and particulates both natural and anthropogenic which are classified as aerosols. Hence the accuracy of the Ancillary data, which is used to estimate the majority of the signal strength from the atmosphere, is critical both to the accuracy of and ability to make retrievals about the ocean contribution from these satellite based measurements at the top of the atmosphere.

The top of the atmosphere reflectance as measured by the satellite is usually partitioned (Gordon & Wang 1994) into its constituent contribution as follows,

$$\rho_t(\lambda) = \rho_r(\lambda) + \rho_A(\lambda) + t(\lambda)\,\rho_w(\lambda) \quad (1)$$

where the three parts refer to the Raleigh scattering from molecules, scattering from aerosols in the atmosphere and the final term denoting the water leaving radiances factored with the transmission through the atmosphere all the way to the top where it is measured. The Atmospheric correction is estimated using wavelength bands where the contribution from the third term is assumed to be zero. Of the two terms left in the equation the Raleigh term dominates in the blue region (80%) and in the NIR region it is close to 50% of the signal. The rest is from the Aerosol contribution. There are published works on improving the estimation of the Raleigh term. M. Wang (2002) has reported on the errors introduced in using the incorrect surface roughness information while estimating this contribution in detail for various bands and a range of wind speeds. This modified method of calculating the Raleigh lookup tables used in the processing is now incorporated in the standard product processing. Any under estimation or overestimation of this contribution due to wrong input values for the sea roughness condition as measured by wind speed values, will affect what fraction of signal measured at the top of the atmosphere is attributed to the remaining part of Aerosol contribution. This has implications for calculating the total aerosol optical depth, which in turn gets used in

determining cloud free pixels using a simple threshold criterion by the cloud algorithm. Hence, a better choice of data inputs used to estimate the Raleigh contribution can definitely improve the products created at NOAA CoastWatch.

All Ocean Color processing algorithms require as input various ancillary data like Atmospheric pressure, water vapor, wind speed and Ozone which make the minimal dataset used to correct for the various contributions of the atmosphere effects to the measured radiances observed at the top of the atmosphere. In addition quantities like wind speed are also used to estimate the sun glint contamination for the observed pixel due to specular reflection at the water surface. The potential sources for the Ancillary data are the monthly climatology for the required parameters or the definitive observations of the state of the atmosphere made for the co-located day and time of the satellite data observation. The directly observed in-situ data footprint as well as from various types of sources (buoys, ships of opportunity, other satellite derived quantities) will be sparser by definition and not always available in a timely manner for all regions of the globe. Hence, the current operational Ocean Color products at NOAA, which are made in near real time (within 12 hours of data acquisition by the satellite) uses monthly climatology as input for the Ancillary datasets. The science quality reprocessed data archived at NASA GSFC uses the definitive Ancillary data, which is created with a lag of a few days from the time of observation. The NASA Ancillary data is also an assimilated data product which uses the NCEP GFS nowcast (McClain et al). It has also been noticed that the total number of successful retrievals from the reprocessed science quality data is usually higher than the one using climatology as input due to static nature of the masking introduced by the use of climatology data, which is not accurately representative of the evolving conditions at the location and time of the satellite observation. To improve the quality of the retrievals made in our operational near real time stream we investigated alternative approaches to the use of monthly climatology, which are currently readily available for use and closely replicates the science quality stream maintained at NASA.

Alternatives to Climatology for Ancillary

One of the alternative schemes investigated initially was the use of the most recent NASA Ancillary data set available closest to the day of satellite data observation from the NASA Ocean Biology Processing Group (OBPG) archive, which usually can be at least a day old. There have been noticeable exceptions to this when Ancillary data files were not available for over 3-5 days. In the case of Ozone data this has been noticed more often than for the other three meteorological parameter files kept in the archive. Hence, we evaluated the use of 1-day old, 2-day old and 5-day old Ancillary data from the NASA archives and compared them with the definitive Ancillary data for all days in the study period. We used the data from the year 2007, and the four seasons picked for this study were represented by the months of January, April, July and October in the evaluation process.

The second scheme investigated was the NCEP generated GFS (Global Forecast Model) data available locally at NOAA. All forecast models are essentially a time integration of the state of the atmosphere represented by the model equations, given the initial conditions of the atmosphere are known as accurately as possible. The state of the atmosphere is represented in physical processes like clouds, precipitation, heat transfer, moisture, momentum and radiation transfer within the model. Improving on these modeled processes and increasing the ensemble size to represent the full subspace of fast growing perturbations using the technique of bred forecasts described in (Toth and Kalnay, 1993 & 1997) as well as increasing power of the supercomputers used has resulted in increasing forecast skill over the years. The GFS model forecast skill for a 36 hour advance forecast approaches the ideal score of 20% over North America at 500 hPa, and is only slightly lower at 30% for a mean sea-level forecast. [E. Kalnay, et al.] As mentioned earlier the initial conditions are extremely important for a good forecast, and are a subject of its own and there are different well known methods already in use to do Data Assimilation. Some of them are SCM, Optimal Interpolation, variational methods in 3D and 4D and Kalman Filter techniques. The data assimilation process uses both the observations available within a window (usually +/-3 hr) along with the regional forecast

value as a first guess. Statistical Interpolation and balancing creates the setup for the initial conditions. This is then fed in to the forecast model to capture the evolution of the atmospheric state for the forecast period.

Various upgrades to the GFS Model have been added over the years and an exhaustive list of the changes (http://www.emc.ncep.noaa.gov/modelinfo/) can be found in the NCEP website. The current model resolution has been increased to T382L64 out to 180hours and T190L64 out to 384 hours. The L64 refers to the number of layers of the atmosphere in the model for which forecast value is available and the T384 refers to the spectral resolution of the model. The number 384 refers to the wave number where the spherical harmonics truncates in the model. At the equator this translates to ~ 45 km for the horizontal resolution of the grid. This is then re-projected to a 1^0 x 1^0 Cartesian grid which is the resolution for all input data in this analysis. For all practical purposes T384 indicates a resolution of 1^0 which is ~ 100 km in cell size whereas the pixel size of satellite measurements is ~ 1 km.

The definitive Ancillary files that NASA uses for reprocessing are actually the NCEP GFS nowcasts which are reformatted with some conversion for use by the NASA Ocean Color processing stream within the SeaWiFS Data Processing Software (SEADAS) suite developed by the OBPG at NASA GSFC. These forecast files are generated 4 times daily (at 00z, 06z, 12z & 18z) for the three meteorological parameters used in Ocean Color processing and twice daily (00z & 12z) in the case of Ozone. These forecast products for a given day are available as early as 384 hours or 16 days in advance, with forecast skill diminishing with lag. We have limited our investigation to forecast model values with a lag of up to 24 hrs, considering that we get to choose from a total of 8 and 4 forecast files for the meteorological parameters and ozone respectively, and they are adequate for our use in near real time processing. For the purpose of evaluation with respect to the NASA definitive Ancillary data for this scheme, we were limited to the use of GFS model forecast data from the year 2008 when this analysis was initiated and due to the rolling archives available at NCEP for the near real time forecast data limited to three months at present.

Currently, the NASA Ancillary data source for Ozone is the TOAST (Total Ozone Analysis using SBUV/2 and TOVS) product from NOAA. This a combination product comprising satellite observations from the two different platforms with radiances in UV bands (252- 340 nm) as well as the 9.7 micron band from TOVS, which is sensitive to ozone retrievals in the 4km to 23 km range. Since the SBUV/2 data collected over 14 orbits per day has data gaps, spatial smoothing is implemented using the Cressman interpolation scheme. This is essentially the replacement for TOVS climatology used in earlier total Ozone column products to represent the mid-to-upper stratosphere (24 to 54 km). Note that the same TOAST product is also used as input to the GFS model as part of the data assimilation process.

Similarly, for the meteorological data inputs the sources are QuikSCAT winds at 0.5 degrees, AMSU-A channels 12 and 13 from NOAA-15 and NOAA-16 and HIRS from NOAA-16, Aqua AIRS and Aqua AMSU-A data, NCEP's new Land Surface Model (Noah LSM) and various other Rawinsonde, ships, aviation (METAR) measurements from regular and data of opportunity sources as well as non-US satellite platforms like METOP, MTSAT and METEOSAT etc are also included in the assimilation. A full list of all such sources can be found at the NCEP webpage containing the GFS data dump text. [http://www.nco.ncep.noaa.gov/pmb/nwprod/realtime/gfs/t00z/index.summary.shtml]

Analysis using old Ancillary data from NASA

In this section we present results from the analysis of Ancillary data for the four seasons and regions using retrospective data from the year 2007 which are available for download from the OBPG archives (http://oceancolor.nasa.gov/). The results show that for all the four input Ancillary parameters there is incremental degradation in using previous few days definitive Ancillary data as a substitute for the current day. This is very acute in the case of Ozone, as shown in the plots from Figs 1-4, the differences can be as large as 10-40 Dobson units for the total column Ozone measurement when using previous days definitive Ancillary as a substitute for measurements for a given day. This is always true

for all regions studied and for all the days for each of the seasons. The evolution of Ozone fronts are also not captured adequately while using the older data as a substitute, as Ozone is a rapidly evolving parameter with time. Since atmospheric correction algorithms are very sensitive to absorption by Ozone, this scheme will make for a poor substitute to climatology, though it may do much better than just using the monthly climatology data as a substitute to the actual total columnar Ozone concentration values for the region of observation.

Similar analysis was also done for the rest of the Ancillary data. The sensitivity to using previous day's values varies. The spread in values as characterized by the standard deviation of the differences is found to be more for the wind speed. The results given below are for the relative differences between the 1-day, 2-day and 5-day old wind speed values when compared with the definitive values for the current day. The relative error can be as high as 60% of the mean wind speed value, which is typically around 3-5 m/s. The seasonal dependence for most regions shows that the differences for wind speed values are the least in the month of July. For the rest of the two meteorological parameters used in Ocean Color processing, Water Vapor and Atmospheric pressure we see that the latter is less sensitive to the choice of day as representative of the current state of the Atmosphere. We do see that the absolute difference and the standard deviation are of the same order of magnitude and in the range of 5 to 10 kg m^{-2}. Water Vapor has the least errors in the summer season, while using this scheme of one day old data as the representative one, for at least three of the regions studied. In the case of Atmospheric pressure we see the least spread in values using the one day old retrievals as a substitute for the day of satellite observation. The relative errors are very low in the less than 1% range largely for all seasons as well as the regions. The absolute value of the differences introduced in this scheme is less than 10 hPa (millibars), and the standard deviation is also as low as 1-5 hPa.

This is the least sensitive of all the four Ancillary parameters required by the Ocean Color processing algorithms. It is also to be noted that the absolute as well as relative errors for the Pressure is lowest for the July season for all the regions except Hawaii

where it is true for both July as well as the month of October. Also note that we found the greatest deviation when using this method for wind speed, which as already discussed before has deeper significance to the accuracy of the Atmospheric correction estimation.

Comparison of Ancillary data sources for Yr 2008

Given below are a summary of the results from the analysis completed for the four seasons and four regions chosen for this study. All data used in this study are for standard CoastWatch regional boxes ref. figure 1, where the land masks are applied, to filter out the land pixels for analysis. We chose to use the bias and the standard deviation of the difference between a given model and the benchmark dataset for Ancillary, as a measure to compare and rank the performance of each Ancillary data source. The relative error is also used when necessary to further illustrate the merits of a given scheme.

The NASA definitive Ancillary that OBPG uses for their science quality reprocessing is set as the standard benchmark to compare all the alternative data streams available for use in L1 to L2 processing. The differences in the values as given by,

$$\text{Ancil Difference} = \text{Ancil}_{\{\text{GFS, Climatology}\}} - \text{Ancil}_{\{\text{NASA}\}} \quad (1)$$

for each pixel in the four CoastWatch region boxes are used to create a composite mean value of the absolute difference for each day of the month as well as the standard deviation of the absolute differences of all the pixels for that day and for each region and season. Further, using these statistical mean values for each day, a grand average for all days of the month is calculated. Each point in the plots in figures 18-21 corresponds to this mean value of the standard deviation for a given season and given region for the various sources of Ancillary input data studied.

For all the three meteorological parameters used we can clearly see that the GFS model forecast values for the T00z and T12z show the smallest spread from the science quality

Ancillary data. Climatology data consistently shows the largest spread from the benchmark values. Even the 1-day and 2-day old definitive NASA Ancillary data is a poorer approximation to the science quality benchmark data and performs worse than the GFS model forecast values. We see no seasonal dependence in the GFS model forecast values, whereas Climatology and one-day old Ancillary data from NASA show poorer performance for the months of January and October for wind speed and pressure values.

In the case of wind speed we see a regional dependence, with the west coast showing slightly larger difference compared to the other regions. Water Vapor shows higher values for July for all regions except Hawaii. The Atmospheric Pressure values from the GFS forecast data seems to show no such dependence and seem to correlate strongly with the science quality Ancillary data.

The retrieval values for Ozone in the GFS model forecasts show the maximum spread from the NASA definitive Ancillary, both seasonally as well as regionally. From Figure 21 it is clear that climatology shows the largest Absolute differences in the total Ozone retrieval as seen by the large spread in the difference with TOAST data for at least two seasons for regions at higher latitudes, which in our case corresponds to the Northeast and West coast CoastWatch boxes. Even the one day old NASA science data will not capture the evolution of the Ozone very well as inferred from the same figure. The regions of Hawaii and Gulf of Mexico show the least sensitivity to Ozone evolution. The difference we see in the GFS Ozone model values is at the 5-10 % level. There are recent unpublished studies available which show that the GFS ozone product has some systematic errors at this level in agreement with what we have observed.

We see from the values in the table 1 above for the Ozone differences that the bias is still large with the GFS model forecast values, when compared to the one-day old OBPG product. The standard deviation values for the GFS forecast product do decrease when compared to Climatology as well as the one-day old definitive Ancillary data. The Bias still remains significant for the forecast product values. The Climatology values are always much lower than the NASA definitive values derived from the TOAST product,

whereas the GFS forecast values for Ozone are biased slightly higher than the NASA distributed TOAST derived product.

From the Table 2 on differences in the wind speed values of the NCEP GFS forecast model and comparing with Climatology product and the one-day old NASA Ancillary shows that the Bias decreases considerably when using the GFS forecast data, especially the nowcast product T12F00F24. Even though the one-day old NASA Ancillary data also has a lower Bias value when compared with the definitive Ancillary for the given day, it does introduce a large scatter in the data as the standard deviation value is much larger than even the 24 hr old forecast data in the last column. At the individual pixel level this could be an issue, so the GFS forecast data proves to be more representative of the day than the other choices available for wind speed values. Just as mentioned earlier the sensitivity of this parameter in Raleigh scattering correction estimation will determine the choice of Ancillary data source. Climatology wind speed differences for all regions and seasons, show large mean values of a factor of 100 more than the differences when using NCEP GFS forecast and this could trigger the cloud algorithm to mask out more pixels as cloud.

The Climatology Ancillary data show the largest bias with respect to the NASA OBPG definitive Ancillary for Water Vapor, for all seasons and regions studied. The Bias value is lowest for the T12F00F24 GFS forecast data and so is the standard deviation too. The Standard deviation when using the 1-day old NASA Ancillary data is as comparable as the Climatology datasets irrespective of the season or region. Though the Bias value increases with the forecast lag as seen in the last two columns of table 3, for the 12 hr and 24 hr advance forecasts (T00F12F36 and T12F24F48) when compared with the 1-day old NASA Ancillary listed in the second column of the same table, the standard deviation is still low for all the NCEP GFS forecasts.

From the above Table 4 for Atmospheric pressure data, we see that the Bias is reduced significantly while using the NCEP GFS forecast data, when compared with Climatology or even lower depending on forecast lag to using the 1-day old NASA Ancillary data. We

do see a substantial improvement in the standard deviation while using the GFS forecast data compared with both the Climatology and 1-day old NASA Ancillary for all regions and seasons and even with increasing forecast lags.

From the summaries given in the above three tables classified by region and season it is clear that NCEP GFS does very well overall for all three metrological parameters Pressure, Water Vapor and Wind speed which are critical in calculating the Atmospheric correction contribution to the top of the Atmosphere radiances measured, before they can be used in empirical band ratio algorithms for estimating the Chlorophyll concentration values to be used in various applications of Remote Sensing of the oceans.

We could alternatively summarize the results by taking aggregate statistical estimates averaged over all the four seasons and various regions to further reduce the information contained in tables 1-4 for the Ancillary data bias and standard deviation. In the case of Ozone we see that the mean value of the bias with Climatology is 14.27±10.69 Dobson units. This reduces further to 2.47±6.02 Dobson units when using GFS forecasts data with up to 24 hour forecast lag. It is to be noted that the GFS data bias for Ozone is higher than when using a one day old definitive Ancillary which is at 0.26±0.53 Dobson units. At this point the source of this larger bias in the forecast data is not entirely understood and will need investigation which is outside the scope of our study. This can have implications for the nLw 531 and 551 nm band values, which is the most sensitive to the presence of Ozone as they are close to the Ozone absorption bands. Even though the mean value of the bias is higher, one also needs to pay attention to the scatter in the Ozone data due to the day-to-day rapid evolution of Ozone concentration for any given pixel location. This is captured well by the standard deviation value estimated for all pixels. The aggregate means for all regions and seasons gives a value of 10.39±4.51 Dobson units for the spread in the case of Climatology data, a lower value of 7.14±4.00 Dobson units when using one-day old definitive Ancillary data from OBPG and an even lower value of 5.82±2.24 Dobson units when using GFS forecast data. The lower scatter in the forecast data even when using data with a 24 hour forecast lag indicates that it captures the evolution of Ozone concentration better than the other two options with

significant improvement over Climatology both for the bias and standard deviation introduced.

In the case of wind speed we see that the Climatology product yields a mean bias value lower at -3.61±2.08 ms^{-1} than the definite NASA OBPG Ancillary used as a benchmark in the comparison. The one-day old NASA Ancillary has a mean bias of 0.01±0.05 ms^{-1} which is again lower like in the case of Ozone. The GFS forecast at smallest lag gives a mean bias of -0.06±0.08 which is again lower than the definitive value for the day. It progressively gets worse and if averaged over three increasing forecast lags, gives a value of -0.14±0.11 ms^{-1} which is still better than what Climatology yields. From the table 2 for wind speed statistics it is clear that one needs to also give weight to the evolution of the winds since it can occur at rapid time scales, at a much faster rate than Ozone changes for a given pixel when selecting one method over the other. The associated uncertainty estimates need to be understood as the variation in the data from changing seasons and regions. The mean value of the standard deviation of the wind speeds are 2.28±0.68 ms^{-1} for Climatology data, slightly lower at 1.80±0.55 ms^{-1} for one-day old NASA Ancillary data and even lower at 0.23±0.16 ms^{-1} for GFS forecast data with no lag (T12F00F24). Hence, this shows that the GFS forecast captures the evolution at the pixel level adequately. If one includes the data with the longer forecast lag then the mean increases to 0.61±0.17 ms^{-1}, which is still lower than the one-day old ancillary and significantly better than using Climatology data which poorly estimates the evolution of wind speed values.

Atmospheric pressure is also an important parameter used in the Raleigh scattering computation by the Atmospheric correction algorithm. The mean values for the bias averaged over seasons and regions in the case of Climatology is -0.62±1.52 millibars, which reduces to 0.04±0.25 millibars for one-day old NASA ancillary data and is 0.10±0.24 millibars for GFS forecast data averaged over three different lag periods. Climatology seems to underestimate the pressure like in the case of other variables. The mean value of the standard deviation is 2.38±1.43 millibars in the case of Climatology; it gets slightly better at 1.99±1.31 millibars for one-day old NASA ancillary and is

0.14±0.06 millibars in the case of GFS forecast with zero lag (T12F00F24) and only increases to 0.28±0.09 millibars when averaged over increased lag periods of up to 24 hours which indicates that GFS data has better performance in capturing the variability in the Atmospheric pressure.

In the case of Water Vapor the aggregate statistics over seasons and regions gives a mean bias of -2.89±1.96 kg m^{-2} in the case of Climatology, which improves to a lower value of -0.09±0.22 kg m^{-2} when using one-day old NASA ancillary and is the best at -0.01±0.06 kg m^{-2} with the NCEP GFS forecast dataset T12F00F24. If one were to average over different forecast lags then one gets a mean bias value of -0.25±0.17 kg m^{-2} better than the Climatology value. Similarly, the metric for the scatter introduced by using different methods is captured by the standard deviation statistic. Averaging this quantity from the table for water vapor, we get the mean value to be 4.38±0.70 kg m^{-2} in the case of Climatology, which increases slightly to a value of 4.59±0.98 kg m^{-2} for one-day old ancillary from NASA and gives the best result for the GFS forecast data T12F00F24 at 0.40±0.12 kg m^{-2}. Including the forecast data up to a 24 hour forecast lag (T12F24F48) we get a value of 1.16±0.24 kg m^{-2} which is still much better than what we currently use in monthly Climatology. As was said in the previous sections the uncertainty estimates associated with the mean values for the bias and the standard deviation is mainly due to the variability across seasons and regions studied being at different latitudes.

So, overall the GFS forecast data with forecast lags and valid for up to 48 hours going forward in time, seem to capture the evolution of all the four Ancillary input parameters: total ozone column density, wind speeds, water vapor and atmospheric pressure used in the Atmospheric correction algorithms much better than the monthly Climatology data.

Validation of GFS model Ancillary for Ocean Color processing

Results from the initial validation work completed by CoastWatch on the new stream of Ocean Color processing planned for the Chesapeake Bay region (to be extended to all

the CoastWatch regions in future) using the GFS model NRT Ancillary products from NCEP is being presented here. We chose to study 4 separate regions (Northeast, Gulf of Mexico, West Coast and Hawaii) as well as four months January, April, July and October representing the seasons. For the Northeast region (NE) we included all available granules for all the days of the each of the representative months in this study. We reprocessed MODIS Aqua L1B radiance calibrated data ordered manually from the NASA data archive (WIST) {https://wist.echo.nasa.gov/api/}. For other regions only three representative days the first, middle and last day of the month were studied to limit the processing and storage space required on our processing machine.

For each granule we processed the L1B data using climatology, NASA definitive Ancillary data as well as the GFS model forecast products from the NCEP data server. For the final analysis we limited ourselves to just the 00hr, 24hr and 48hr forecast model products to reduce workload and diminishing returns. The additional two model products are also for the 00hr and 24hr forecasts with a 12hr time lag. NCEP makes predictions every 6 hrs for the MET parameters used in Ocean Color processing (wind speed, Atmospheric pressure, water vapor) and for Ozone there are two predictions made daily.

The results are presented below as various plots. We studied the chlorophyll as well the water leaving radiance values (nLws: 412, 443, 488, 531, 551, 667 nm) for all the chosen days after creating the daily composites from the individual granules. Time series plots of the daily composite differences for each and every pixel were also done to see the extent of the outliers not captured by aggregate statistics like mean and standard deviation. From the aggregate statistics for daily products a monthly average for each and every region and season was created and written out in ASCII as a text file. These summary files were later used to create the summary plots shown in figures 22-32.

We also created subsets for the Chesapeake Bay region from the Northeast CoastWatch box. The results for this region is of immediate interest, since we plan to use the GFS forecast data for the Ocean Color processing for this region as a trial run before applying the same method to other CoastWatch regions. Based on the results so far, we

recommend the use of NCEP GFS model forecast data for the four parameters (Ozone, wind speed, pressure and water vapor) used in Ocean Color processing as a replacement for the monthly climatology data that is being currently used in the near real time processing stream at NOAA. With this replacement we expect to improve the quality of retrievals when compared to our present products and closely match the values of our products to the science quality reprocessed data from NASA. We present below results which show that our products with the new set of Ancillary datasets will be on average within less than ±5% for the Chesapeake Bay region, both for the normalized water leaving radiance values (nLw) as well as for the derived Chlorophyll concentration values.

Summary of Results:

In this section we summarize the results from the validation study using the NCEP GFS forecast data processed Ocean Color products for all seasons. In the case of North East and its subset the Chesapeake Bay region the data sampling included all days of the representative months. For the other regions we limited the sampling to just three days for each month, as a result the summary statistics could show large outliers. Since, it was shown earlier in the section on Ancillary data analysis that all regions showed improvement with the GFS forecast data at the input level when compared to using Climatology data, we can safely presume that this improvement carries over to the L2 products produced using the forecast data. Some of the measures like the relative error of the Chlorophyll are shown for all regions in the table 3. The relative error is defined as,

$$\text{Relative Error (Chlor)} = (\text{Chlor}_{GFS} - \text{Chlor}_{OBPG}) / \text{Chlor}_{OBPG} \quad (2)$$

Using this measure, the chlorophyll concentration product using the NCEP GFS forecast model data as inputs used in the Near Real Time (NRT) processing shows a maximum difference of ~ 10% for the 24 hr advance forecast model run, when compared to the science quality reprocessed OBPG product stream. This is a remarkable improvement

when compared with Climatology processed NRT products where the Relative error can be as high as ~ 70% for the North East region in winter month of January. Similar results for the nLw values are shown in the next section with figures for the North East and its subset, the Chesapeake Bay region.

The mean value of the Chlorophyll concentration values derived for each of the regions and seasons are shown in Fig 24 for comparison. The Chesapeake Bay region being mostly coastal waters and within estuaries the retrieval values show a larger mean value for each season. The other four regions cluster around a band of values. We also estimated the mean bias for each season and region normalized to the mean seasonal values for each region to arrive at the Relative Bias which is shown below in Figure 25.

In the next section we show the comparison results using the nLw bands (412nm, 443nm, 488nm, 531nm, 551nm & 667 nm) using similar definitions for the measure.

$$nLw\_diff\ (\lambda) = nLw\ (\lambda)_{GFS} - nLw\ (\lambda)_{OBPG} \qquad (3)$$

And for the error measure we have the usual definition where the difference as mentioned in the equation (2) above is normalized to the nLw value obtained for that band from the science quality reprocessing stream $nLw(\lambda)_{OBPG}$, where λ denotes the band.

$$\text{Relative Error } (nLw(\lambda)) = (nLw(\lambda)_{GFS} - nLw(\lambda)_{OBPG}) \ / \ |\, nLw(\lambda)_{OBPG} \,| \qquad (4)$$

Note, that in calculating the relative error for the nLw values, since nLw values after the atmospheric correction can be negative one needs to normalize the differences with the absolute value to avoid dilution of the sign in the end result.

As we can see from the above table containing the Bias and Standard deviation of the chlorophyll differences that, with increasing lags in the model forecast Ancillary used in the processing, a small degradation is observed in both the bias and standard deviation, but it is still much smaller than the bias and standard deviation seen while using

Climatology for the Ancillary data. The drop in bias values is by almost a factor of 10 in both the North east and the smaller Chesapeake Bay region averages for all seasons. For the other regions the same result holds and in the case of Hawaii the bias values are an order of magnitude lower than for the other regions with the standard deviation remaining almost the same.

From the tables (7 & 8) above for the North east region, the Absolute Relative errors in the nLw values estimated in the NRT stream using GFS model inputs, for all the relevant six bands except the nLw_667 band for the North east region do show that it is no more than 5 % at the extreme. Most values are in the 2 % to 3 % different from the science quality reprocessed values for the 443 nm, 488 nm, 531 nm and 551 nm bands used in the empirical band ratio Chlorophyll algorithms.

The relative errors for the Chesapeake Bay region's nLw values (Table 9) for all the bands decreases for the NCEP GFS generated values compared with Climatology, for all the seasons. The drop in the relative difference is most significant for the blue bands 412 nm and 443 nm, from as high as ~50 % for Climatology to ~10 % when using the latest GFS forecast data.

In the tables (8 & 10), we show the Bias and the standard deviation of the differences in the nLw values computed for all the six bands (412nm to 667nm). We see again some improvement in the standard deviation values with the GFS forecast compared to the Climatology, though the bias values do not show such a behavior in the data. There is a band, region and season dependence and no clear pattern emerges, though the GFS Ancillary data use does not particularly degrade the value of the nLw retrievals in general.

From the table summarizing the data for the Gulf of Mexico in Table 11, we see that the standard deviation for the nLw differences using GFS forecasts made up to 48hr in advance is smaller than that for the cases using Climatology as Ancillary data for all seasons and regions. In the case of Bias this is true most of the time but not always with

some bands and seasons showing more sensitivity to the GFS model forecast. This could be a result of sampling errors, since we limited ourselves to only three representative days for the other regions. Similar results are seen also for the West Coast and Hawaii mostly. The Bias and Standard deviation of the difference for all the nLw bands decrease with the NCEP GFS forecast data as Ancillary.

Taking averages for all seasons and regions in the table of relative errors for the derived Chlorophyll values, for each of the different Ancillary streams we see that the Absolute relative errors seem a good statistic to characterize the maximum difference. Climatology data usage yield a mean value for the relative error of 9.6%, whereas the GFS model forecast gives mean values of 6.7-8.3 % depending on the forecast lag. Since, we are aware of a few outliers in the data as evidenced in the table, the corresponding median values for the relative error are 4.3% for Climatology data and in the range 2.2-2.5% for GFS model data. If the same exercise is repeated for the signed value of the relative error the respective mean values is 8.6% for Climatology and 5.3-7.3% for GFS model data. The corresponding median values are 3.6% and 0.65-1.2 %.

Similarly, the mean values for the bias in the case of climatology use comes out to be 0.049; whereas the mean value of the bias for GFS model usage is in the range of 0.015-0.018 a factor of 4-5 less showing considerable improvement with forecast data. The corresponding median values for the bias are 0.025 and 0.005 for climatology and GFS model, which clearly shows the same factor of difference and closing in on the accuracy of the measurements itself at the low end of the Chlorophyll concentration. The mean values for the standard deviation of the signed differences give a value of 1.31 for Climatology and in the range 1.004-1.11 for the GFS model use. The corresponding median values are 1.16 for Climatology and 0.96-1.01 for the GFS model. A few order of magnitude larger standard deviation values over the bias, indicates the large variation in the valid values for Chlorophyll which also spans a few orders of magnitude. It should also be noted that the region definitions used are also large and encompass coastal as well as open ocean waters.

For the nLw values we can also compute an average value for the relative errors for all season of a given region from the tables (8 & 9). The Climatology mean relative error for the Northeast region is around 6.59% and it reduces to 3.76% when using GFS model forecast for Ancillary data. The mean values for the standard deviation of the relative error is 7.05% and 3.47% respectively for Climatology and the GFS model data, indicating a spread in the relative error of the same order as the error itself. It has to be noted that the 412 nm and the 667nm band show larger relative errors which skews the average value higher. These bands are not used in the band ratio empirical algorithms used for calculating the Chlorophyll concentration. In the case of the subset of this region around the Chesapeake Bay the mean value of the relative error increases as expected for Climatology stream to 11.55% and for the GFS forecast data it is 6.16%, a factor of two more than when averaged over open ocean waters. However, the mean of the standard deviation values for this region, are 11.33% and 5.2% respectively for Climatology and GFS forecasts. This also shows that the mean and standard deviation values for the relative error are comparable for both region classifications. It is of significance to note that with the GFS forecast data as Ancillary, we have reduced the relative errors to around 6% or less, when compared with the use of Climatology data. If one excludes the 412 nm and 667nm band from this average computation then we will likely yield a value much less than 5%. It is ~ 3.4% for GFS use in the Chesapeake Bay region and 7.9% for Climatology data use. The same numbers for the Northeast region is 1.9% and 3.67%. This shows a very good agreement with the NASA OBPG derived science quality nLw values for those critical bands for the proposed NRT data stream and is quite encouraging.

The data in the tables for the bias and standard deviation of nLw values from GFS model and Climatology when compared with the science quality OBPG data can be further summarized to arrive at some interesting results. Like we did before, taking the average over all seasons and all the nLw bands for the Northeast region alone, we get a mean value of the bias for the GFS forecast data as 0.0015 ± 0.0009 mW sr^{-1} cm^{-2} μm^{-1} and for the Climatology data the mean value of the bias is -0.0035 ± 0.006 mW sr^{-1} cm^{-2} μm^{-1} which shows that the nLw values are on average lower when using Climatology which

will lead to overestimation of Chlorophyll in the band ratio algorithms, since lower water leaving radiance implies more absorbing pigments in the water column. Restricting the mean value computation to the four bands 443, 488, 531 and 551 nm only, changes the mean value of the bias to 0.0016 mW sr^{-1} cm^{-2} μm^{-1} and -0.002 mW sr^{-1} cm^{-2} μm^{-1} for GFS and Climatology respectively. The GFS mean bias value is very stable as measured by the low value of the spread in the bias at 0.0009 mW sr^{-1} cm^{-2} μm^{-1} whereas for Climatology it is an order higher at 0.006 mW sr^{-1} cm^{-2} μm^{-1}.

Another interesting statistic to consider would be the aggregate standard deviation of the differences for all pixels in a region enumerated for each of the nLw band by season and model Ancillary used and do a comparison to get at the underlying spread in values at the resolution of a pixel level. The mean value for the standard deviation of all pixels for the Northeast region studies yields a value of 0.0267±0.011 mW sr^{-1} cm^{-2} μm^{-1} in the case of GFS model forecast and a higher value of 0.038±0.018 mW sr^{-1} cm^{-2} μm^{-1} in the case of Climatology indicating that the GFS model is a closer approximation to the science quality processing stream. There seem to be not much difference in the spread in the standard deviation values for all seasons and bands between the different Ancillary streams, though the mean value of the standard deviation for all data is higher in the case of Climatology.

Similar exercise for the Chesapeake Bay a subset of the Northeast region which is mostly coastal waters and estuaries would be also very illustrative. From the table 10 for the Bay, we estimate the mean value of the bias to be 0.0059±0.0031 mW sr^{-1} cm^{-2} μm^{-1} for the GFS model data and -0.0027±0.0053 mW sr^{-1} cm^{-2} μm^{-1} for the Climatology data. We see here again that the Climatology nLw mean bias is negative, indicating an underestimation of the water leaving radiance overall which can lead to higher Chlorophyll values in the estuaries and coastal regions. The GFS mean bias is also higher for the Chesapeake Bay subset when compared to the larger Northeast region, so also is the spread of the mean values for the region subset; the GFS data still yields a slightly lower spread in the mean bias when compared to Climatology always even with the region subset. Restricting the mean computation again to only the four bands (443nm to

551nm) like before, gives mean bias values of 0.0061 mW sr^{-1} cm^{-2} μm^{-1} and -0.0019 mW sr^{-1} cm^{-2} μm^{-1} for GFS and Climatology respectively. The aggregate values for the standard deviation of the differences for all pixels, when averaged over all seasons and nLw bands gives, a larger value of 0.0389±0.0134 mW sr^{-1} cm^{-2} μm^{-1} for the GFS data and 0.0529±0.0191 mW sr^{-1} cm^{-2} μm^{-1} for the Climatology data. This is higher than values in the previous paragraph for the larger area representing the Northeast data and is expected of coastal waters where there is a larger variability due to constituent loading of the water from land based effluents as well as the atmospheric contamination from aerosols other than of marine origin. Excluding the 412nm and 667nm band from this calculation does not change the mean value of the standard deviation by any significant amount for the limited Chesapeake Bay region like with the case of the larger Northeast box.

For the other regions we studied due to limited number of days included in the study we summarize only the absolute relative error estimates for the nLw values when using Climatology and GFS model data. For the West Coast region the mean value of the relative error for nLw is 3.624±4.397 % with the GFS data when compared with 6.834±4.707 % when using Climatology. For the four central bands this number further reduced to 1.54 % and 4.23 % respectively. The lower latitude regions like the Gulf of Mexico have mean values for the relative error at 2.88±3.76 % and 4.84±6.15 % for GFS and Climatology data when used. For Hawaii which is largely open ocean water, the values drop further to 0.95±1.68 % and 2.24±4.11 % respectively. The associated uncertainty values given with the relative error estimates are the standard deviation of the mean relative error when averaged over the bands and seasons. When the above estimates are limited to the central bands the corresponding value drop to 0.243 % and 0.619 % for Hawaii, 0.89 % and 1.55 % for the Gulf of Mexico region. This indicates that large uncertainty in the aggregated means is mostly due to the 412 nm and 667nm bands returning larger relative errors as seen in the tables 14-16 for the absolute relative errors and not entirely due to contributions from seasonal changes.

Chlorophyll image comparison

We compare below images from figures 30, 35 of the processed Ocean color data with the various schemes analyzed above as input for Ancillary data. From the Chlorophyll image comparisons for the month of April (figure 35) one can tell that the NCEP-GFS is closer to the science quality data stream produced at NASA than the NOAA NRT products created using Climatology datasets for Ancillary. It is quite prominent in the case of Northeast data for the month of April (figure 38). The top row of this figure shows the Climatology Ancillary created product, the middle row shows the one created using NASA OBPG Ancillary data and the bottom row ones using NCEP GFS Ancillary data. For April which is the second column in the collection, the waters off the Newfoundland coast show large Chlorophyll concentration values when compared to science quality processed images. This could probably be explained by the large uncertainty in nLw values introduced for pixels with large solar zenith angles and large sensor viewing angles with incorrect wind speed values as explained in the paper by M. Wang (2002) on Raleigh lookup tables used in Atmospheric correction processes.

We also analyzed the region of immediate interest the Chesapeake Bay region images. Difference images of the monthly composite Chlorophyll image product with the science quality stream using NASA Ancillary is given in the figures 33-37. We do see improvement in the retrieval values for Chlorophyll when the processing uses the GFS forecast products for the Ancillary data over climatology (figures 34 and 35). We also see some degradation in the product quality when forecast data with a more than 48 hrs lag (figure 37), is used in the processing. In real time data processing, we would limit ourselves to at most 24-hr old forecast data for Ancillary, since we have at least 4 choices per day to select from, and it is very unlikely that the 48 hr forecasts will be used in near real time processing.

For the other regions studied, since the processing was limited to representative samples of three days from each season we do not present the difference images due to the sparse data in the image map. We shall present those results in a summary tabular format for

reference. The mean value of the Chlorophyll difference is approximately ~ 0.03 mg m^{-3} in the open ocean waters and 0.1 mg m^{-3} in the estuaries and coastal waters. The standard deviation of the Chlorophyll retrievals is approximately in the range 0.4 – 1.0 mg m^{-3} for the Northeast region depending on the season. In the case of the Chesapeake Bay region it increases to a mean value of 0.027 to 0.096 mg m^{-3} and the standard deviation ranges from values of 1.5 to 3.7 mg m^{-3}. It has the highest variability in summer as seen in the July data from the summary on Chlorophyll statistics Table 6.

We also studied the nLw values for the Northeast region and the results from that analysis is summarized below as a time series of the difference between the NCEP GFS processed retrievals with that from the NASA OBPG science quality Ancillary processed retrievals for all the ocean bands of Aqua. Of these the 531nm and the 551nm bands are the most sensitive to ozone and hence of interest. The absolute differences in the nLw values are not more than 0.005 (mW cm^{-2} sr^{-1} μm^{-1}) for 443nm and 488nm bands and it is less than 0.01 (mW cm^{-2} sr^{-1} μm^{-1}) for the 531nm and 551nm bands most sensitive to Ozone absorption.

Case study Day106

We observe that our current standard Ocean Color product which uses climatology for Ancillary does have some oddities when compared with NASA OBPG produced products for the same day. One such example we shall discuss in some detail is for day 106 of 2009 for the Northeast region. We noticed that a large number of pixels were being flagged as cloud pixels close to shore as well as out to open ocean waters. There were no nLw values reported for these pixels as they were getting masked by the cloud algorithm at the L1B to L2 stage itself.

We processed this particular granule (MODIS file: MODSCW_P2009106_1800) in question using three difference streams of Ancillary data, just as was discussed in the seasonal study. We found that the only stream where this masking was getting introduced

was while using Climatology Ancillary datasets. We then further investigated the individual ancillary parameters and made difference maps for each parameter. For this granule, the Climatology Ozone differences in the sub region of the granule in question were the least when compared to definitive ancillary values from the OBPG set. But we did find differences in the wind speed to be large while using climatology. There is already a published work by M. Wang [78] which shows the sensitivity of the radiances calculated assuming zero wind speed, in the NIR bands for different wind speed values. It has been shown there that the delta-L change to radiance is negative for the 869 nm bands with increasing wind speed values. So when using climatology data which always has lower mean values for the wind speed, the expected correction for the Rayleigh scattering is a smaller quantity, leaving a larger part for the rest of the total radiance measured at the top of the atmosphere, left to be accounted for by aerosols of various kinds which also include clouds. Note that the 869 nm band reflectance is used by the cloud mask algorithm with a threshold value of 0.027 to trigger the cloud mask. The difference map of the rho_869 band values between climatology and NASA reprocessed science quality data do not entirely account for this underestimate. As seen in the figure 48 it does not recreate the contours of the cloud mask seen in the chlorophyll image.

There could be other effects which are more dominant in this particular case. For the day in question climatology wind speed values for the pixels in question are very low when compared to the ambient wind conditions. This in effect means that the correction for the atmosphere contribution part through the Raleigh scattering term as shown in equation (1) is under evaluated leaving large uncorrected values for the total TOA radiance in the 869nm band. The low wind speed values have another important effect, that of under accounting for the sun-glint. It has already been well established that lower wind speed in certain ranges for the sensor viewing angles, leads to lower estimates for the sun glint radiance [Wang and Bailey 2001]. This again implies that for those pixels the glint correction applied is lower than for the ambient higher wind speed conditions with associated sun glint. The 869 nm band reflectance is left with a value higher than the threshold value set at 0.027 for the cloud mask to be flagged for those pixels. This is well illustrated in the figure 49 which shows the delta_869, defined to be the value of the

reflectance above the threshold of 0.027. For those regions where the glint correction value is lower than this difference delta_869, the under-correction still leaves those pixels with positive residuals above the threshold for determining presence of cloud.

The image map of the sunglint radiance, tLg_869 and the respective difference maps for climatology and NASA definitive reprocessing shown in figures 50-52 further corroborate the fact that the glint contribution is underestimated in the case of Climatology. As seen in the images of chlorophyll processed with Climatology, NASA OBPG and NCEP GFS Ancillary data the contour of the cloud masks overlap the region of rhos_869 above threshold (fig 49) and difference in glint radiance (fig 52). Further the image maps of the glint coefficient for the two separate cases processed using different ancillary data show significant difference. What is interesting to also note is that the rhos_869 reflectance is not very different between data processed with the two ancillary streams indicating that the glint correction is not applied to the surface reflectance values at the top of the atmosphere (TOA) as expected though the corrected values are assumed to be used by the cloud masking algorithm. This example clearly illustrates the case why there is a need to use the NCEP GFS Ancillary data in our near real time products, to keep as many good pixels as possible which are critical for our users.

Conclusions:

The current usage of Climatology Ancillary data in operational Ocean Color processing is shown to introduce large errors in the Chlorophyll concentration retrieval values which are used for many useful routine forecasts like the Harmful algal bloom products. Amongst the alternative schemes explored we have shown conclusively that the NCEP GFS model forecast values for the Ancillary data necessary improves substantially the retrieval values for Ocean Color and brings it closer to the baseline retrieval values from the reprocessing done using definitive Ancillary datasets at NASA. We also show that the minimal impact to the quality of retrieval values are ensured by using the nowcast data when available or any forecast data within a 24hr lag window from the time of observation of the satellite data. Further, since the masking for clouds and other ambient

conditions is more representative while using the GFS forecast data when compared with climatology, thereby resulting in increasing the number of successful retrievals and overall product quality improvements in the near real time Ocean Color processing stream.

Acknowledgements

This work was supported by NOAA funds through the activities within the CoastWatch program in NESDIS/STAR. We also would like to acknowledge the efforts of our colleague Phillip Keegstra in making available elements of the modified processing software as used in CoastWatch for near real time processing adapted to ingesting NCEP GFS forecast model data. We would also like to acknowledge the use of CDAT data analysis toolset from CoastWatch which was also used in this analysis. We would also like to express our gratitude for access to the MODIS Aqua L1B calibrated data from the NASA/GSFC data archives. The views, opinions and results contained in this paper are solely of the authors and not to be construed as an official NOAA policy position on the matter presented.

Table 1 Ancillary data (Ozone) difference:

Bias & Standard Deviation of the Difference ($Ozone_{[Clim, 1day, GFS]} - Ozone_{OBPG}$)

Stdev is measured with NASA OBPG Ancillary as baseline value in Dobson units

Region	Season	Climatology	1-day lag	T00F00F18	T12F12F30	T00F24F42
NE	Jan	15.82 ± 17.11	1.16 ± 11.11	10.03 ± 8.70	10.84 ± 9.80	11.64 ± 10.21
	Apr	39.01 ± 17.53	0.19 ± 10.49	7.37 ± 6.33	5.91 ± 6.62	5.90 ± 6.89
	Jul	22.43 ± 9.58	0.07 ± 4.05	3.43 ± 4.14	3.18 ± 4.54	1.89 ± 4.34
	Oct	1.65 ± 8.77	1.39 ± 6.83	1.61 ± 5.77	0.94 ± 5.30	0.61 ± 5.50
GM	Jan	13.03 ± 5.41	0.24 ± 3.45	0.24 ± 3.73	-1.42 ± 3.96	-1.59 ± 3.89
	Apr	23.17 ± 9.16	0.77 ± 3.48	3.26 ± 3.26	2.72 ± 3.48	2.53 ± 3.54
	Jul	11.53 ± 8.14	0.15 ± 5.11	-3.46 ± 5.20	-3.79 ± 5.46	-3.97 ± 5.80
	Oct	7.98 ± 6.45	-0.28 ± 4.11	-5.22 ± 3.92	-5.22 ± 3.91	-5.42 ± 3.90
WC	Jan	1.53 ± 17.39	-0.08 ± 14.35	12.78 ± 10.55	11.18 ± 10.61	12.86 ± 10.76
	Apr	23.08 ± 17.73	-0.38 ± 15.76	10.66 ± 9.21	11.44 ± 9.79	9.48 ± 9.63
	Jul	28.91 ± 10.24	-0.08 ± 6.54	7.94 ± 5.87	7.26 ± 5.58	5.89 ± 5.46
	Oct	8.05 ± 9.12	0.71 ± 9.96	0.02 ± 5.41	0.02 ± 5.59	-1.39 ± 5.72
HI	Jan	8.52 ± 7.90	0.19 ± 4.87	3.20 ± 4.70	5.83 ± 5.40	5.09 ± 5.45
	Apr	15.65 ± 10.69	0.37 ± 6.29	2.39 ± 5.12	3.99 ± 5.80	3.76 ± 5.92
	Jul	5.84 ± 5.61	0.29 ± 3.01	-5.54 ± 3.23	-4.76 ± 3.51	-4.82 ± 3.67
	Oct	2.10 ± 5.39	-0.51 ± 4.80	-7.27 ± 4.67	-6.24 ± 4.64	-7.18 ± 4.90

Table 2 Ancillary data (Wind Speed) difference:

Bias & Standard Deviation of the Difference (Wind speed $_{[Clim, 1day, GFS]}$ − Wind speed$_{OBPG}$)

Stdev is measured with NASA OBPG Ancillary as baseline value in ms^{-1}

Region	Season	Climatology	1-day lag	T12F00F24	T00F12F36	T12F24F48
NE	Jan	-5.43 ± 2.65	-0.03 ± 2.72	-0.03 ± 0.11	-0.56 ± 1.02	-0.40 ± 1.21
	Apr	-6.33 ± 2.90	-0.08 ± 2.20	-0.04 ± 0.14	-0.26 ± 0.86	-0.17 ± 1.18
	Jul	-3.21 ± 2.06	-0.04 ± 1.56	0.01 ± 0.09	-0.15 ± 0.81	0.05 ± 1.00
	Oct	-6.64 ± 2.79	0.11 ± 2.26	-0.01 ± 0.10	-0.37 ± 0.88	-0.13 ± 1.08
GM	Jan	-4.80 ± 2.59	-0.02 ± 2.05	-0.08 ± 0.25	-0.42 ± 0.81	-0.39 ± 0.93
	Apr	-3.23 ± 2.00	-0.01 ± 1.63	-0.06 ± 0.17	-0.22 ± 0.69	-0.09 ± 0.81
	Jul	-2.06 ± 1.73	0.07 ± 1.16	-0.06 ± 0.13	-0.19 ± 0.61	-0.09 ± 0.75
	Oct	-2.95 ± 1.81	0.08 ± 1.47	-0.03 ± 0.21	-0.25 ± 0.79	-0.14 ± 0.88
WC	Jan	-6.91 ± 3.75	0.02 ± 2.62	-0.22 ± 0.57	-0.22 ± 0.78	-0.15 ± 1.01
	Apr	-3.84 ± 2.58	-0.02 ± 2.11	-0.12 ± 0.45	-0.17 ± 0.63	-0.18 ± 0.91
	Jul	-1.58 ± 1.97	-0.01 ± 1.76	-0.05 ± 0.41	-0.03 ± 0.58	-0.01 ± 0.75
	Oct	-4.40 ± 3.04	0.01 ± 2.44	-0.23 ± 0.53	-0.25 ± 0.77	-0.11 ± 1.01
HI	Jan	-3.86 ± 2.34	0.01 ± 1.31	-0.05 ± 0.15	-0.19 ± 0.53	-0.20 ± 0.68
	Apr	-0.98 ± 1.54	-0.01 ± 1.24	0.03 ± 0.16	-0.001 ± 0.51	-0.09 ± 0.76
	Jul	0.06 ± 1.15	0.05 ± 0.97	0.01 ± 0.13	-0.05 ± 0.45	-0.09 ± 0.57
	Oct	-1.53 ± 1.53	0.06 ± 1.34	0.003 ± 0.14	-0.08 ± 0.51	-0.06 ± 0.74

Table 3 Ancillary data (Water Vapor) difference:

Bias & Standard Deviation of the Difference (Water Vapor $_{[Clim, 1day, GFS]}$ − Water Vapor$_{OBPG}$)

Stdev is measured with NASA OBPG Ancillary as baseline value

Region	Season	Climatology	1-day lag	T12F00F24	T00F12F36	T12F24F48
NE	Jan	-2.14 ± 4.43	-0.10 ± 5.66	-0.06 ± 0.37	-0.32 ± 0.96	-0.47 ± 1.44
	Apr	-3.97 ± 5.05	-0.09 ± 5.50	-0.07 ± 0.49	-0.36 ± 1.17	-0.61 ± 1.80
	Jul	-4.99 ± 5.08	0.12 ± 5.51	-0.11 ± 0.69	-0.28 ± 1.76	-0.57 ± 2.67
	Oct	0.39 ± 4.96	-0.74 ± 5.74	0.08 ± 0.51	-0.05 ± 1.31	-0.06 ± 1.96
GM	Jan	-3.47 ± 4.59	-0.10 ± 5.38	-0.01 ± 0.44	-0.54 ± 1.18	-0.51 ± 1.82
	Apr	-4.09 ± 4.48	-0.28 ± 4.68	0.06 ± 0.44	-0.31 ± 1.28	-0.57 ± 1.79
	Jul	-4.56 ± 4.60	-0.01 ± 3.80	0.11 ± 0.33	-0.55 ± 1.39	-0.54 ± 1.95
	Oct	-3.03 ± 5.74	-0.35 ± 6.23	0.04 ± 0.29	-0.59 ± 1.45	-0.99 ± 2.33
WC	Jan	0.93 ± 3.18	-0.03 ± 3.95	-0.002 ± 0.22	-0.19 ± 0.81	-0.31 ± 1.27
	Apr	-1.09 ± 3.02	0.02 ± 3.83	0.02 ± 0.26	-0.34 ± 0.80	-0.42 ± 1.26
	Jul	-5.09 ± 4.61	-0.02 ± 4.08	-0.03 ± 0.33	-0.58 ± 1.22	-0.53 ±1.73
	Oct	-1.64 ± 4.03	-0.12 ± 4.92	-0.01 ± 0.27	-0.09 ± 0.99	-0.04 ± 1.64
HI	Jan	-1.52 ± 3.72	-0.11 ± 3.54	0.04 ± 0.40	-0.36 ± 1.24	-0.11 ± 1.92
	Apr	-5.88 ± 4.48	0.18 ± 3.03	-0.07 ± 0.46	-0.43 ± 1.24	-0.15 ± 1.77
	Jul	-3.71 ± 4.09	0.11 ± 3.48	-0.07 ± 0.44	-0.63 ± 1.32	-0.31 ± 1.93
	Oct	-2.31 ± 3.97	0.04 ± 4.09	-0.03 ± 0.46	-0.26 ± 1.46	0.02 ± 2.26

Table 4 Ancillary data (Pressure) difference:

Bias & Standard Deviation of the Difference (Pressure $_{[Clim, 1day, GFS]}$ − Pressure$_{OBPG}$)

Stdev is measured with NASA OBPG Ancillary as baseline value

Region	Season	Climatology	1-day lag	T12F00F24	T00F12F36	T12F24F48
NE	Jan	-2.929 ± 3.261	0.195 ± 4.298	0.164 ± 0.198	-0.156 ± 0.401	-0.031 ± 0.560
	Apr	-1.418 ± 3.087	-0.491 ± 3.015	0.133 ± 0.197	0.008 ± 0.344	0.123 ± 0.564
	Jul	0.558 ±1.803	-0.259 ± 1.411	0.035 ± 0.115	-0.005 ± 0.288	0.333 ± 0.440
	Oct	-1.489 ± 2.670	0.589 ± 2.690	0.081 ± 0.137	-0.192 ± 0.305	-0.163 ± 0.430
GM	Jan	-0.533 ± 2.011	-0.204 ± 1.941	0.122 ± 0.162	-0.013 ± 0.249	0.094 ± 0.342
	Apr	0.589 ± 1.428	0.011 ± 1.173	0.050 ± 0.090	-0.313 ± 0.245	-0.216 ± 0.308
	Jul	0.855 ± 1.082	-0.090 ± 0.738	-0.059 ± 0.072	-0.357 ± 0.238	-0.445 ± 0.350
	Oct	-1.774 ± 1.265	0.386 ± 0.875	0.011 ± 0.098	-0.280 ± 0.222	-0.362 ± 0.295
WC	Jan	1.698 ± 6.384	0.237 ± 4.356	0.226 ± 0.229	0.421 ± 0.474	0.709 ± 0.659
	Apr	-1.823 ± 3.067	0.105 ± 2.846	0.342 ± 0.220	0.275 ± 0.348	0.008 ± 0.505
	Jul	2.492 ± 2.926	0.085 ± 2.051	0.428 ± 0.218	0.465 ± 0.344	0.515 ± 0.446
	Oct	-1.168 ± 4.030	-0.080 ± 3.497	0.251 ± 0.208	0.143 ± 0.358	-0.057 ± 0.583
HI	Jan	-2.600 ± 2.075	0.125 ± 0.786	0.013 ± 0.087	0.094 ± 0.210	0.306 ± 0.325
	Apr	-0.594 ± 1.204	-0.048 ± 0.836	0.051 ± 0.091	0.183 ± 0.202	0.245 ± 0.310
	Jul	-0.215 ± 0.887	0.051 ± 0.562	0.099 ± 0.078	0.358 ± 0.201	0.606 ± 0.277
	Oct	-1.526 ± 0.977	0.094 ± 0.773	0.073 ± 0.080	0.149 ± 0.179	0.362 ± 0.284

Table 5 Chlorophyll Relative Error: ($Chlor_{GFS} - Chlor_{OBPG}$) / $Chlor_{OBPG}$

The absolute value of the relative error is also given within brackets.

Region	Season	Climatology (%)	T00F12F24 (%)	T00F36F48 (%)	T00F60F72 (%)
NE	Jan	70.58 (71.49)	31.80 (32.53)	41.92 (42.6)	35.53 (36.14)
	Apr	7.03 (7.62)	0.93 (1.91)	0.67 (2.15)	0.81 (2.80)
	Jul	3.60 (4.28)	1.14 (2.23)	0.90 (2.40)	1.08 (2.62)
	Oct	4.16 (6.52)	1.73 (3.42)	1.90 (3.75)	2.02 (4.03)
GM	Jan	4.17 (4.38)	0.30 (1.12)	0.62 (1.14)	0.51 (1.28)
	Apr	3.13 (3.88)	1.79 (2.26)	2.01 (2.76)	1.88 (2.49)
	Jul	0.80 (1.24)	0.09 (1.68)	0.35 (1.98)	0.22 (1.77)
	Oct	2.57 (5.05)	2.55 (4.77)	0.98 (3.13)	0.34 (2.27)
WC	Jan	45.99 (47.38)	93.63 (93.76)	53.99 (54.29)	54.45 (54.71)
	Apr	3.18 (3.42)	1.17 (1.42)	1.18 (1.64)	0.78 (1.59)
	Jul	2.55 (2.75)	0.58 (0.91)	0.11 (0.66)	0.09 (0.60)
	Oct	2.52 (3.83)	1.49 (3.21)	1.81 (3.90)	1.17 (3.68)
HI	Jan	0.21 (0.99)	0.40 (0.48)	0.40 (0.62)	0.27 (0.46)
	Apr	2.16 (2.22)	-0.08 (0.48)	0.07 (0.60)	0.15 (0.52)
	Jul	3.92 (5.45)	0.52 (2.25)	0.26 (1.90)	0.46 (2.25)
	Oct	-0.06 (0.30)	-0.41 (0.46)	-0.48 (0.50)	-0.45 (0.45)
CY	Jan	4.28 (7.71)	3.44 (4.50)	3.18 (4.38)	5.87 (7.06)
	Apr	3.53 (4.01)	1.73 (1.73)	0.05 (2.25)	-0.02 (2.60)
	Jul	4.69 (5.44)	2.64 (4.33)	1.42 (3.55)	1.60 (3.51)
	Oct	2.35 (4.98)	-0.10 (2.54)	-0.44 (2.45)	0.02 (2.52)

Table 6 Bias & Stdev of the Chlorophyll differences: ($Chlor_{GFS} - Chlor_{OBPG}$)

Region	Season	Climatology	T00F12F24	T00F36F48	T00F60F72
NE	Jan	0.026±0.536	0.012±0.389	0.014±0.421	0.017±0.453
	Apr	0.115±1.419	0.023±0.989	0.016±1.103	0.022±1.131
	Jul	0.030±1.156	0.007±1.087	0.009±1.149	0.012±1.168
	Oct	0.024±1.159	-0.002±0.694	-0.003±0.839	0.001±0.856
GM	Jan	0.011±0.353	0.004±0.259	0.004±0.347	0.005±0.389
	Apr	0.073±2.410	-0.0003±1.52	-0.007±1.624	-0.013±2.138
	Jul	0.008±0.963	0.007±0.939	0.007±0.825	0.006±0.941
	Oct	0.018±1.339	-0.005±1.037	-0.007±1.118	-0.005±1.171
WC	Jan	0.009±0.199	0.009±0.168	0.007±0.165	0.007±0.195
	Apr	0.047±2.272	0.006±1.697	0.005±1.755	0.0004±2.059
	Jul	0.025±1.616	0.004±1.218	0.004±1.056	0.004±1.081
	Oct	0.007±0.598	-0.004±0.377	-0.007±0.399	-0.008±0.480
HI	Jan	-0.0002±0.002	0.0001±0.002	0.0001±0.002	0.0001±0.001
	Apr	0.0013±0.006	0.0000±0.003	0.0002±0.003	0.0002±0.0032
	Jul	0.0019±0.010	-0.0003±0.003	-0.0002±0.003	-0.0003±0.003
	Oct	-0.00005±0.001	-0.0001±0.001	-0.0002±0.001	-0.0002±0.001
CY	Jan	0.097±1.808	0.065±1.468	0.078±1.659	0.133±1.679
	Apr	0.169±3.139	0.096±2.524	0.094±2.915	0.061±2.831
	Jul	0.203±3.943	0.048±3.684	0.068±3.591	0.089±3.471
	Oct	0.112±3.214	0.027±2.022	0.021±2.103	0.038±2.103

Table 7 Absolute Relative errors (%) for the nLw values for the North East region

Region	Season	Climatology	412nm (%)	443nm (%)	488nm (%)	531nm (%)	551nm (%)	667nm (%)
NE	Jan	Climatology	**11.25**	**9.03**	**2.32**	**5.05**	**8.23**	**27.81**
		T00F12F24	3.19	2.47	0.85	2.24	3.88	12.48
		T00F36F48	4.22	3.52	1.09	2.67	4.49	14.15
		T00F60F72	6.10	4.51	1.41	3.05	4.86	16.60
	Apr	Climatology	**15.61**	**7.22**	**2.08**	**2.19**	**2.69**	**20.82**
		T00F12F24	4.74	1.98	0.85	0.93	1.12	8.12
		T00F36F48	6.67	2.83	1.07	1.12	1.32	9.37
		T00F60F72	7.74	3.68	1.35	1.41	1.65	11.99
	Jul	Climatology	**4.50**	**2.11**	**1.10**	**1.34**	**1.81**	**11.12**
		T00F12F24	2.57	1.23	0.79	0.97	1.25	7.68
		T00F36F48	2.84	1.53	0.96	1.16	1.47	9.47
		T00F60F72	3.01	1.63	1.02	1.19	1.50	9.66
	Oct	Climatology	**18.09**	**6.90**	**2.01**	**2.21**	**2.54**	**16.51**
		T00F12F24	4.08	1.79	0.52	0.74	0.97	6.30
		T00F36F48	5.99	2.36	0.67	0.85	1.06	6.91
		T00F60F72	7.15	2.95	8.35	0.99	1.22	8.31

Table 8 Bias & Standard deviation for nLw values in the Northeast region

Region	Season	Climatology	412nm	443nm	488nm	531nm	551nm	667nm
NE	Jan	Climatology	-0.0002±0.0568	-0.0003±0.0465	0.0022±0.0352	0.0061±0.0356	0.0068±0.0355	0.00167±0.0162
		T00F12F24	0.0007±0.0286	0.0005±0.0250	0.0012±0.0208	0.0028±0.0211	0.0031±0.0209	0.0007±0.0109
		T00F36F48	0.0020±0.0319	0.0015±0.0276	0.0020±0.0229	0.0038±0.0233	0.0041±0.0232	0.0009±0.0116
		T00F60F72	0.0031±0.0375	0.0023±0.0322	0.0028±0.0263	0.0049±0.0269	0.0053±0.0269	0.0012±0.0128
	Apr	Climatology	-0.0149±0.0712	-0.0113±0.0590	-0.0042±0.0416	0.003±0.0339	0.0045±0.0325	0.0011±0.0141
		T00F12F24	0.0012±0.0402	0.0011±0.0343	0.0011±0.0256	0.0014±0.0199	0.0016±0.0185	0.0004±0.0086
		T00F36F48	0.0019±0.0482	0.0016±0.0404	0.0012±0.0297	0.0011±0.0229	0.0011±0.0211	0.0003±0.0096
		T00F60F72	0.0006±0.0599	0.0007±0.0510	0.0006±0.0378	0.0005±0.0287	0.0005±0.0265	0.0002±0.0118
	Jul	Climatology	-0.0152±0.0630	-0.011±0.0522	-0.005±0.0359	0.001±0.0252	0.0018±0.0238	0.0005±0.009
		T00F12F24	0.0035±0.0499	0.0031±0.0439	0.0026±0.0336	0.0023±0.0251	0.0023±0.0234	0.0008±0.0103
		T00F36F48	0.0026±0.0593	0.0026±0.0520	0.0023±0.0393	0.0019±0.0291	0.0019±0.0271	0.0008±0.0116
		T00F60F72	0.0021±0.0621	0.0021±0.0545	0.0019±0.0413	0.0016±0.0306	0.0016±0.0284	0.0008±0.0124
	Oct	Climatology	-0.0189±0.0682	-0.0143±0.0535	-0.0079±0.0365	-0.0045±0.0287	-0.0034±0.0259	-0.0009±0.0128
		T00F12F24	0.0015±0.0254	0.0010±0.0209	0.0003±0.0159	-0.0003±0.0137	-0.0004±0.0128	-0.0001±0.0071
		T00F36F48	0.0026±0.0299	0.0019±0.0244	0.0008±0.0179	-0.0001±0.0148	-0.0003±0.0137	-0.0001±0.0075
		T00F60F72	0.0016±0.0350	0.0010±0.0283	0.0002±0.0203	-0.0005±0.0165	-0.0006±0.0151	-0.0002±0.0081

Table 9 Absolute Relative Errors in nLw values for the Chesapeake Bay

Region	Season	Climatology	412nm (%)	443nm (%)	488nm (%)	531nm (%)	551nm (%)	667nm (%)
CY	Jan	Climatology	**50.66**	**26.58**	**11.33**	**12.57**	**14.54**	**30.07**
		T00F12F24	12.16	9.19	2.26	2.63	2.99	17.25
		T00F36F48	15.54	12.21	3.01	3.63	4.08	12.31
		T00F60F72	21.29	13.22	4.25	5.27	5.91	26.41
	Apr	Climatology	**17.40**	**7.93**	**2.60**	**1.93**	**1.84**	**6.54**
		T00F12F24	5.23	2.61	0.80	0.76	0.69	3.56
		T00F36F48	6.82	2.96	0.85	0.78	0.80	3.69
		T00F60F72	8.47	3.68	1.07	0.86	0.88	5.58
	Jul	Climatology	**26.29**	**10.64**	**2.63**	**1.61**	**1.71**	**14.62**
		T00F12F24	10.72	5.14	2.63	2.21	2.42	16.85
		T00F36F48	11.31	8.25	3.18	2.55	2.79	18.23
		T00F60F72	10.58	7.74	2.91	2.25	2.43	16.32
	Oct	Climatology	**40.33**	**19.66**	**4.59**	**3.30**	**3.15**	**10.93**
		T00F12F24	15.55	7.38	1.54	0.99	0.97	2.81
		T00F36F48	15.84	7.68	1.38	1.03	1.03	3.06
		T00F60F72	17.23	7.80	1.75	1.08	1.02	3.53

Table 10 Bias & Standard deviation of nLws for the Chesapeake Bay region

Region	Season	Climatology	412nm	443nm	488nm	531nm	551nm	667nm
CY	Jan	Climatology	-0.002±0.089	-0.003±0.081	0.001±0.066	0.007±0.059	0.009±0.056	0.002±0.032
		T00F12F24	0.006±0.049	0.004±0.046	0.005±0.039	0.008±0.034	0.009±0.031	0.002±0.0198
		T00F36F48	0.009±0.053	0.007±0.049	0.007±0.041	0.010±0.036	0.011±0.033	0.002±0.021
		T00F60F72	0.009±0.056	0.007±0.052	0.009±0.043	0.015±0.039	0.017±0.037	0.003±0.022
	Apr	Climatology	-0.0150±0.060	-0.0130±0.055	-0.0080±0.044	-0.001±0.035	0.0001±0.032	-0.0003±0.017
		T00F12F24	-0.0002±0.034	-0.0002±0.031	-0.0005±0.025	-0.001±0.019	-0.001±0.0176	-0.0003±0.009
		T00F36F48	-0.0003±0.038	-0.0003±0.036	-0.0009±0.029	-0.002±0.002	-0.002±0.020	-0.0005±0.011
		T00F60F72	0.001±0.046	0.001±0.042	-0.001±0.033	-0.002±0.026	-0.003±0.024	-0.001±0.013
	Jul	Climatology	-0.007±0.078	-0.005±0.072	-0.0003±0.058	0.005±0.045	0.006±0.041	0.002±0.022
		T00F12F24	0.018±0.078	0.017±0.073	0.014±0.060	0.012±0.047	0.012±0.043	0.005±0.022
		T00F36F48	0.0197±0.086	0.0187±0.080	0.0160±0.066	0.014±0.051	0.013±0.047	0.006±0.024
		T00F60F72	0.0197±0.085	0.0186±0.080	0.0157±0.066	0.013±0.051	0.013±0.047	0.013±0.047
	Oct	Climatology	-0.013±0.079	-0.011±0.073	-0.007±0.058	-0.005±0.048	-0.005±0.043	-0.001±0.026
		T00F12F24	0.009±0.046	0.007±0.042	0.003±0.034	0.001±0.028	0.0003±0.026	-0.0003±0.016
		T00F36F48	0.008±0.046	0.006±0.042	0.002±0.034	0.000±0.027	-0.001±0.025	-0.0004±0.016
		T00F60F72	0.004±0.050	0.003±0.046	0.001±0.037	-0.0004±0.029	-0.0001±0.027	-0.0003±0.017

Table 11 Bias & Stdev for the Gulf of Mexico region

Region	Season	Climatology	412nm	443nm	488nm	531nm	551nm	667nm
GM	Jan	Climatology	-0.0201±0.0573	-0.0144±0.0435	-0.0059±0.0249	0.0005±0.0175	0.0021±0.0163	0.0004±0.0075
		T00F12F24	-0.0020±0.0209	-0.0016±0.0176	-0.0008±0.0127	0.00004±0.010	0.0003±0.0095	0.0001±0.0047
		T00F36F48	0.0009±0.0227	0.0008±0.0189	0.0008±0.0136	0.0012±0.0109	0.0012±0.0097	0.0004±0.0053
		T00F60F72	0.0006±0.0252	0.0006±0.0210	0.0007±0.0150	0.0012±0.0123	0.0012±0.0111	0.0004±0.0056
	Apr	Climatology	-0.0136±0.0543	-0.0103±0.0462	-0.0044±0.0335	0.0017±0.0258	0.0026±0.0246	0.0007±0.0119
		T00F12F24	0.0067±0.0380	0.0055±0.0321	0.0041±0.0232	0.0038±0.0174	0.0035±0.0166	0.0008±0.0078
		T00F36F48	0.0055±0.0395	0.0046±0.0334	0.0033±0.0239	0.0027±0.0175	0.0028±0.0168	0.0006±0.0081
		T00F60F72	0.0045±0.0396	0.0039±0.03421	0.0032±0.0255	0.0033±0.0200	0.0035±0.0190	0.0007±0.0101
	Jul	Climatology	-0.0004±0.0399	-0.0001±0.0340	0.0003±0.02483	0.0005±0.0179	0.0007±0.0168	0.0003±0.0075
		T00F12F24	0.0028±0.0313	0.0020±0.0277	0.0008±0.0213	-0.0007±0.0160	-0.0009±0.0152	-0.0001±0.0068
		T00F36F48	0.0041±0.0404	0.0031±0.0359	0.0015±0.0273	-0.0003±0.0202	-0.0006±0.0192	-0.0001±0.0084
		T00F60F72	0.0046±0.0313	0.0035±0.0261	0.0017±0.0017	-0.0003±0.0122	-0.0006±0.0115	-0.0001±0.0046
	Oct	Climatology	-0.0125±0.0554	-0.0104±0.0454	-0.0073±0.0309	-0.0058±0.0229	-0.0054±0.0207	-0.0017±0.0089
		T00F12F24	0.0084±0.0500	0.0052±0.0285	0.0024±0.0195	-0.0002±0.0139	-0.0007±0.0125	-0.0001±0.0059
		T00F36F48	0.0043±0.0295	0.0067±0.0351	0.0034±0.0237	0.0007±0.0168	0.0001±0.0149	0.0001±0.0068
		T00F60F72	0.0065±0.0418	0.0064±0.0409	0.0035±0.0275	0.0014±0.0192	0.0009±0.0171	0.0002±0.0073

Table 12 Bias & Stdev for the West Coast region

Region	Season	Climatology	412nm	443nm	488nm	531nm	551nm	667nm
WC	Jan	Climatology	-0.0199±0.1104	-0.0163±0.0933	-0.0102±0.0703	-0.0056±0.0599	-0.0045±0.0566	-0.0008±0.0235
		T00F12F24	-0.0007±0.0415	-0.0005±0.0406	0.0009±0.0368	0.0037±0.0366	0.0042±0.0365	0.0010±0.0227
		T00F36F48	0.0012±0.0442	0.0011±0.0422	0.0014±0.0370	0.0026±0.0351	0.0029±0.0344	0.0008±0.0224
		T00F60F72	0.0041±0.0528	0.0034±0.0489	0.0029±0.0409	0.0035±0.0375	0.0035±0.0367	0.0009±0.0238
	Apr	Climatology	-0.0073±0.0539	-0.0056±0.0440	-0.0023±0.0302	0.0011±0.0227	0.0018±0.0215	0.0005±0.0104
		T00F12F24	-0.0002±0.0185	-0.0001±0.0166	0.0005±0.0137	0.0015±0.0123	0.0016±0.0118	0.0004±0.0066
		T00F36F48	0.0010±0.0221	0.0008±0.0195	0.0009±0.0156	0.0016±0.0138	0.0017±0.0133	0.0004±0.0072
		T00F60F72	0.0025±0.0251	0.0020±0.0216	0.0017±0.0168	0.0018±0.0146	0.0018±0.0140	0.0004±0.0070
	Jul	Climatology	-0.0042±0.0422	-0.0025±0.0340	0.0003±0.0223	0.0032±0.0168	0.0036±0.0162	0.0009±0.0055
		T00F12F24	-0.0010±0.0142	-0.0008±0.0119	-0.0003±0.0082	0.0001±0.0059	0.0002±0.0055	0.0000±0.0023
		T00F36F48	-0.0013±0.0185	-0.0011±0.0155	-0.0006±0.0105	-0.0003±0.0071	-0.0003±0.0066	-0.0001±0.0024
		T00F60F72	-0.0022±0.0188	-0.0017±0.0155	-0.0009±0.0103	-0.0004±0.0068	-0.0003±0.0064	-0.0001±0.0023
	Oct	Climatology	-0.0104±0.0615	-0.0072±0.0475	-0.0037±0.0319	-0.0017±0.0256	-0.0012±0.0239	-0.0001±0.0119
		T00F12F24	0.0016±0.0259	0.0013±0.0220	0.0004±0.0165	-0.0007±0.0141	-0.0009±0.0135	-0.0002±0.0105
		T00F36F48	0.0019±0.0291	0.0014±0.0243	0.0004±0.0178	-0.0009±0.0150	-0.0012±0.0143	-0.0003±0.0083
		T00F60F72	0.0048±0.0503	0.0039±0.0412	0.0019±0.0279	-0.0000±0.0212	-0.0005±0.0196	-0.0004±0.0081

Table 13 Bias & Stdev for the Hawaii region

Region	Season	Climatology	412nm	443nm	488nm	531nm	551nm	667nm
HI	Jan	Climatology	0.0011±0.0178	-0.0008±0.0097	-0.0005±0.0064	-0.0004±0.0059	-0.0004±0.0058	-0.0001±0.0019
		T00F12F24	0.0002±0.0065	0.0002±0.0052	0.0002±0.0033	0.0004±0.0032	0.0004±0.0031	0.0001±0.0010
		T00F36F48	0.0002±0.0056	0.0002±0.0049	0.0002±0.0034	0.0003±0.0036	0.0003±0.0035	0.0001±0.0013
		T00F60F72	0.0003±0.0057	0.0003±0.0049	0.0002±0.0032	0.0002±0.0030	0.0002±0.0028	0.00004±0.0009
	Apr	Climatology	0.0013±0.0172	0.0019±0.0153	0.0022±0.0117	0.0030±0.0110	0.0030±0.0109	0.0008±0.0031
		T00F12F24	0.0001±0.0099	-0.000±0.0076	-0.0001±0.0051	-0.0002±0.0038	-0.0002±0.0036	-0.0001±0.0012
		T00F36F48	0.0007±0.0101	0.0005±0.0084	0.0003±0.0057	0.0001±0.0045	0.0001±0.0044	0.00002±0.0014
		T00F60F72	0.0003±0.0123	0.0003±0.0097	0.0002±0.0064	0.0002±0.0046	0.0002±0.0045	0.00001±0.0014
	Jul	Climatology	0.0105±0.0572	0.0089±0.0469	0.0062±0.0329	0.0049±0.0239	0.0046±0.0220	0.0011±0.0084
		T00F12F24	-0.0087±0.0588	0.0004±0.0306	0.0018±0.02086	-0.0002±0.0129	-0.0008±0.0108	0.0001±0.0032
		T00F36F48	-0.0095±0.0605	-0.0001±0.0315	00016±0.0212	-0.0002±0.0133	-0.0006±0.0111	0.0001±0.0033
		T00F60F72	-0.0098±0.0602	-0.0005±0.0314	0.0013±0.0212	-0.0005±0.0133	-0.0009±0.0112	0.0000±0.0033
	Oct	Climatology	0.0004±0.0135	0.0002±0.0103	-0.0000±0.0057	-0.0001±0.0029	-0.0001±0.0025	-0.0000±0.0009
		T00F12F24	0.0001±0.0017	0.0000±0.0014	-0.0001±0.0012	-0.0004±0.0021	-0.0004±0.0023	-0.0001±0.0006
		T00F36F48	-0.0001±0.0046	-0.0002±0.0038	-0.0003±0.0024	-0.0005±0.0027	-0.0005±0.0028	-0.0001±0.0007
		T00F60F72	-0.000±0.0039	-0.0001±0.0032	-0.0002±0.0022	-0.0004±0.0027	-0.0005±0.0027	-0.0001±0.0007

Table 14 Absolute Relative Error for Hawaii

Region	Season	Climatology	412nm (%)	443nm (%)	488nm (%)	531nm (%)	551nm (%)	667nm (%)
HI	Jan	Climatology	**0.09**	**0.09**	**0.08**	**0.30**	**0.49**	**5.66**
		T00F12F24	0.05	0.05	0.05	0.15	0.23	2.46
		T00F36F48	0.05	0.05	0.05	0.17	0.28	3.23
		T00F60F72	0.05	0.05	0.05	0.14	0.22	2.54
	Apr	Climatology	**0.19**	**0.20**	**0.24**	**0.71**	**1.08**	**10.15**
		T00F12F24	0.06	0.06	0.06	0.17	0.26	2.34
		T00F36F48	0.09	0.08	0.09	0.22	0.34	3.13
		T00F60F72	0.11	0.10	0.10	0.21	0.30	3.79
	Jul	Climatology	**0.96**	**0.91**	**0.88**	**1.87**	**2.62**	**25.28**
		T00F12F24	0.47	0.28	0.30	0.64	0.83	10.11
		T00F36F48	0.54	0.34	0.35	0.69	0.88	10.48
		T00F60F72	0.55	0.35	0.36	0.71	0.90	10.54
	Oct	Climatology	**0.11**	**0.11**	**0.09**	**0.11**	**0.13**	**1.34**
		T00F12F24	0.03	0.04	0.04	0.15	0.23	1.73
		T00F36F48	0.05	0.05	0.05	0.18	0.27	2.26
		T00F60F72	0.06	0.06	0.06	0.17	0.25	2.21

Table 15 Absolute Relative Error of nLw for the West Coast

Region	Season	Climatology	412nm (%)	443nm (%)	488nm (%)	531nm (%)	551nm (%)	667nm (%)
WC	Jan	Climatology	**22.72**	**12.55**	**4.75**	**14.44**	**15.60**	**30.14**
		T00F12F24	3.32	2.56	0.97	4.72	6.98	34.79
		T00F36F48	4.07	3.72	1.13	3.28	5.70	35.08
		T00F60F72	6.37	5.66	1.54	4.66	6.35	40.90
	Apr	Climatology	**7.75**	**3.69**	**1.34**	**1.09**	**1.32**	**9.05**
		T00F12F24	1.98	0.85	0.40	0.46	0.60	4.88
		T00F36F48	2.55	1.05	0.52	0.58	0.76	5.78
		T00F60F72	4.16	1.71	0.74	0.65	0.80	5.83
	Jul	Climatology	**1.29**	**1.02**	**0.64**	**0.94**	**1.25**	**7.57**
		T00F12F24	0.35	0.29	0.18	0.19	0.24	1.60
		T00F36F48	0.40	0.36	0.21	0.23	0.29	1.78
		T00F60F72	0.40	0.35	0.21	0.23	0.28	1.66
	Oct	Climatology	**6.35**	**3.23**	**1.28**	**1.97**	**2.55**	**11.49**
		T00F12F24	2.27	1.54	0.40	0.61	0.85	5.26
		T00F36F48	3.31	2.19	0.54	0.70	0.95	6.18
		T00F60F72	5.29	3.34	0.99	1.15	1.38	8.65

Table 16 Absolute Relative Error of nLw for the Gulf of Mexico

Region	Season	Climatology	412nm (%)	443nm (%)	488nm (%)	531nm (%)	551nm (%)	667nm (%)
GM	Jan	Climatology	**10.76**	**3.16**	**1.06**	**1.24**	**1.54**	**17.82**
		T00F12F24	2.33	0.76	0.38	0.64	0.84	8.64
		T00F36F48	2.89	0.93	0.44	0.61	0.77	8.78
		T00F60F72	2.72	0.86	0.46	0.74	0.95	10.04
	Apr	Climatology	**5.67**	**3.19**	**1.34**	**1.65**	**2.16**	**29.38**
		T00F12F24	2.41	1.35	0.71	1.03	1.39	18.22
		T00F36F48	2.59	1.64	0.74	0.94	1.28	16.52
		T00F60F72	3.33	1.82	0.76	1.00	1.30	23.21
	Jul	Climatology	**0.90**	**0.64**	**0.44**	**0.58**	**0.72**	**5.32**
		T00F12F24	0.58	0.40	0.27	0.41	0.58	4.30
		T00F36F48	0.88	0.56	0.38	0.51	0.67	4.68
		T00F60F72	0.89	0.59	0.39	0.51	0.65	4.69
	Oct	Climatology	**8.21**	**2.52**	**1.19**	**1.54**	**1.89**	**13.12**
		T00F12F24	7.13	1.53	0.65	0.74	0.96	5.65
		T00F36F48	9.01	1.91	0.86	0.96	1.19	7.44
		T00F60F72	9.35	2.21	1.01	1.12	1.34	8.66

Table 17 Signed Relative errors for NE region

Region	Season	Climatology	412nm (%)	443nm (%)	488nm (%)	531nm (%)	551nm (%)	667nm (%)
NE	Jan	Climatology	**-1.19**	**1.75**	**1.22**	**3.81**	**6.66**	**20.56**
		T00F12F24	0.20	0.69	0.60	1.83	3.24	9.89
		T00F36F48	1.44	1.71	0.86	2.29	3.90	11.63
		T00F60F72	1.12	2.67	1.12	2.70	4.34	14.05
	Apr	Climatology	**-8.23**	**-1.18**	**-0.20**	**0.90**	**1.45**	**14.43**
		T00F12F24	1.20	0.64	0.34	0.39	0.50	4.43
		T00F36F48	2.10	1.16	0.36	0.31	0.37	3.99
		T00F60F72	0.69	1.13	0.24	0.16	0.18	3.70
	Jul	Climatology	**-2.94**	**-1.21**	**-0.50**	**0.20**	**0.60**	**5.71**
		T00F12F24	1.29	0.52	0.34	0.38	0.48	4.13
		T00F36F48	1.08	0.53	0.33	0.29	0.38	4.05
		T00F60F72	0.88	0.46	0.27	0.24	0.31	3.52
	Oct	Climatology	**-12.97**	**-2.60**	**-0.87**	**-1.09**	**-1.13**	**-7.07**
		T00F12F24	1.60	0.88	0.14	-0.05	-0.07	0.66
		T00F36F48	2.35	1.17	0.23	0.03	-0.01	1.03
		T00F60F72	1.30	0.54	0.11	-0.08	-0.13	0.40

Table 18 Signed Relative Error for CY05 region

Region	Season	Climatology	412nm (%)	443nm (%)	488nm (%)	531nm (%)	551nm (%)	667nm (%)
CY	Jan	Climatology	**-7.29**	**5.43**	**7.84**	**10.05**	**12.00**	**24.01**
		T00F12F24	4.62	6.19	1.80	2.18	2.53	1.65
		T00F36F48	7.72	8.72	2.51	3.16	3.58	11.10
		T00F60F72	7.87	9.07	3.63	4.75	5.35	25.28
	Apr	Climatology	**-6.81**	**0.25**	**-0.53**	**-0.19**	**-0.06**	**2.32**
		T00F12F24	-0.53	0.79	-0.001	-0.10	-0.14	1.75
		T00F36F48	-1.71	0.90	-0.04	-0.20	-0.16	1.36
		T00F60F72	1.45	1.44	0.02	-0.29	-0.30	2.73
	Jul	Climatology	**-20.30**	**2.61**	**0.24**	**0.61**	**0.93**	**3.15**
		T00F12F24	8.74	4.04	2.00	1.80	2.02	15.57
		T00F36F48	7.95	6.04	2.22	1.87	2.09	14.07
		T00F60F72	5.89	5.42	2.01	1.70	1.89	11.96
	Oct	Climatology	**-26.49**	**-1.41**	**-0.26**	**-0.39**	**-0.33**	**3.23**
		T00F12F24	12.72	5.14	0.84	0.28	0.18	0.53
		T00F36F48	10.25	4.94	0.61	0.03	-0.07	-0.37
		T00F60F72	4.46	2.42	0.34	-0.07	-0.05	0.57

Table 19 Signed Relative errors for Hawaii region

Region	Season	Climatology	412nm (%)	443nm (%)	488nm (%)	531nm (%)	551nm (%)	667nm (%)
HI	Jan	Climatology	**-0.06**	**-0.05**	**-0.04**	**-0.11**	**-0.18**	**-2.28**
		T00F12F24	0.01	0.01	0.01	0.09	0.15	1.76
		T00F36F48	0.007	0.009	0.014	0.06	0.10	1.39
		T00F60F72	0.01	0.01	0.01	0.04	0.07	0.71
	Apr	Climatology	**0.06**	**0.09**	**0.16**	**0.65**	**0.99**	**9.27**
		T00F12F24	0.003	-0.001	-0.001	-0.04	-0.07	-0.24
		T00F36F48	0.03	0.02	0.02	0.02	0.04	0.66
		T00F60F72	0.01	0.01	0.02	0.04	0.06	0.93
	Jul	Climatology	**0.43**	**0.43**	**0.46**	**1.09**	**1.57**	**13.61**
		T00F12F24	-0.34	0.03	0.14	-0.02	-0.21	3.61
		T00F36F48	-0.37	0.01	0.13	-0.002	-0.17	4.18
		T00F60F72	-0.39	-0.01	0.11	-0.06	-0.25	3.48
	Oct	Climatology	**0.01**	**0.01**	**-0.001**	**-0.02**	**-0.04**	**-0.24**
		T00F12F24	0.01	0.005	-0.01	-0.14	-0.22	-1.57
		T00F36F48	-0.01	-0.01	-0.03	-0.18	-0.27	-2.06
		T00F60F72	-0.01	-0.02	-0.03	-0.17	-0.25	-2.09

Table 20 Signed Relative error for West Coast region

Region	Season	Climatology	412nm (%)	443nm (%)	488nm (%)	531nm (%)	551nm (%)	667nm (%)
WC	Jan	Climatology	**-17.98**	**-6.95**	**-3.14**	**-10.09**	**-8.03**	**-2.08**
		T00F12F24	-1.43	0.79	0.62	4.45	6.74	34.21
		T00F36F48	-0.91	1.92	0.75	2.06	4.60	33.10
		T00F60F72	1.59	3.46	1.13	4.35	5.89	39.06
	Apr	Climatology	**-4.18**	**-3.21**	**-1.57**	**2.70**	**5.18**	**5.86**
		T00F12F24	0.98	0.42	0.22	0.33	0.48	3.99
		T00F36F48	1.74	0.66	0.32	0.39	0.53	4.26
		T00F60F72	3.41	1.38	0.55	0.44	0.53	3.61
	Jul	Climatology	**-0.33**	**-0.23**	**0.12**	**0.68**	**0.97**	**6.67**
		T00F12F24	0.003	0.02	0.01	0.03	0.05	0.52
		T00F36F48	-0.04	0.003	-0.05	-0.04	-0.05	-0.01
		T00F60F72	-0.10	-0.05	-0.07	-0.06	-0.08	-0.05
	Oct	Climatology	**-3.68**	**-1.58**	**-0.67**	**-0.85**	**-0.92**	**-0.61**
		T00F12F24	1.09	1.15	0.15	-0.12	-0.24	-0.02
		T00F36F48	2.12	1.56	0.20	-0.17	-0.34	-2.98
		T00F60F72	3.19	2.45	0.46	-0.02	-0.18	-2.81

Table 21 Signed Relative error for the Gulf of Mexico region

Region	Season	Climatology	412nm (%)	443nm (%)	488nm (%)	531nm (%)	551nm (%)	667nm (%)
GM	Jan	Climatology	**-9.82**	**-2.18**	**-0.69**	**0.02**	**0.60**	**12.15**
		T00F12F24	-0.56	-0.22	-0.05	-0.03	-0.01	-0.86
		T00F36F48	0.08	0.20	0.15	0.24	0.35	4.35
		T00F60F72	0.21	0.11	0.13	0.20	0.25	4.74
	Apr	Climatology	**-3.74**	**-0.59**	**-0.28**	**0.26**	**0.63**	**-1.36**
		T00F12F24	1.31	0.96	0.50	0.81	1.12	16.41
		T00F36F48	0.83	1.03	0.40	0.56	0.79	11.44
		T00F60F72	0.45	1.08	0.45	0.72	0.99	19.63
	Jul	Climatology	**0.12**	**0.06**	**0.05**	**0.09**	**0.17**	**2.49**
		T00F12F24	3.23	0.23	0.11	-0.13	-0.25	-2.33
		T00F36F48	0.54	0.35	0.18	-0.01	-0.13	-0.87
		T00F60F72	0.60	0.39	0.20	0.04	-0.08	-0.21
	Oct	Climatology	**-2.19**	**-0.85**	**-0.67**	**-1.01**	**-1.22**	**-7.03**
		T00F12F24	5.99	1.03	0.32	0.02	-0.11	0.01
		T00F36F48	7.75	1.32	0.45	0.21	0.12	1.83
		T00F60F72	7.82	1.46	0.51	0.37	0.34	2.51

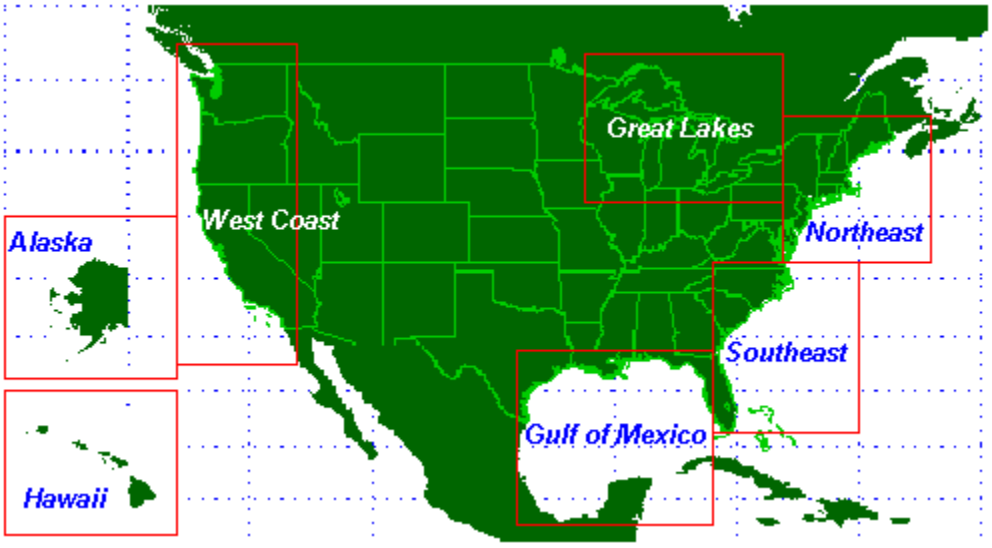

Figure 1 CoastWatch region boxes used in the study were the Northeast, Gulf of Mexico, West Coast and Hawaii

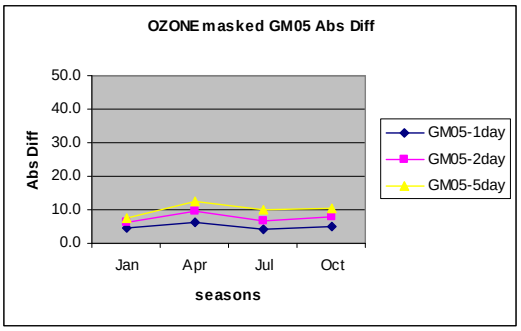

Figure 2 Ozone for the Gulf of Mexico region

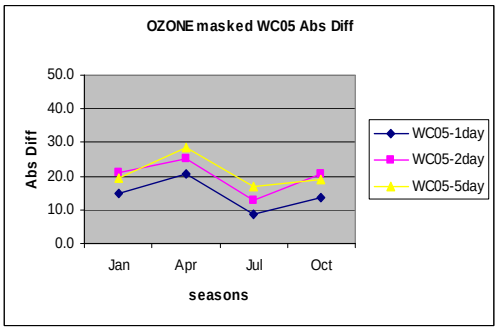

Figure 4 Ozone for the West Coast region

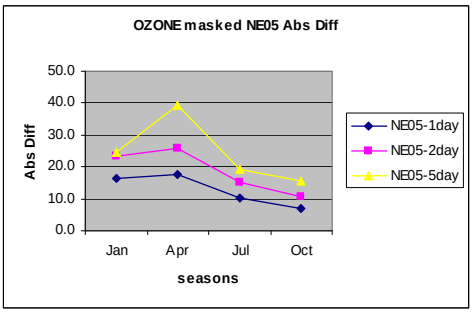

Figure 3 Ozone for the Northeast region

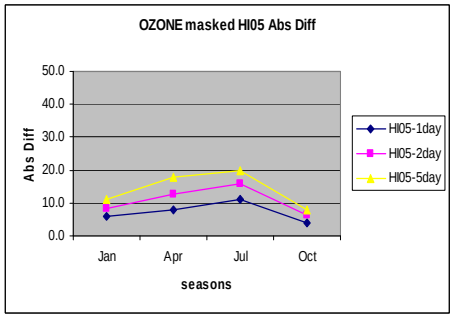

Figure 5 Ozone for the Hawaii region

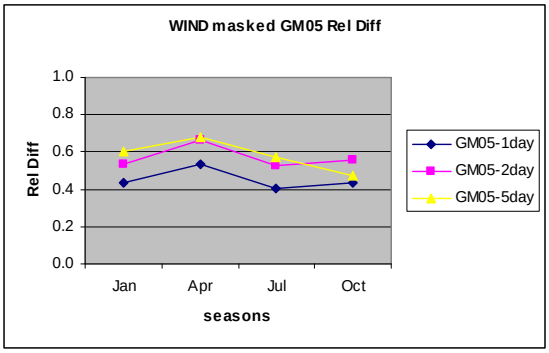

Figure 6 Wind Speed Relative error for Gulf of Mexico region

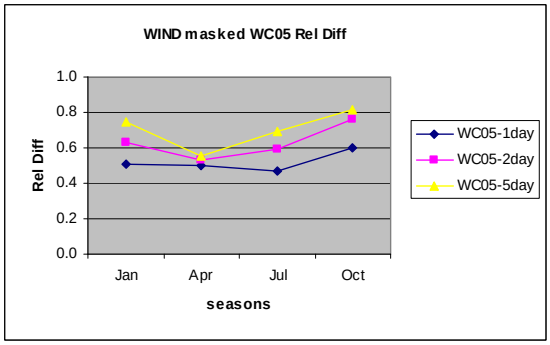

Figure 8 Wind speed Relative error for the West Coast region

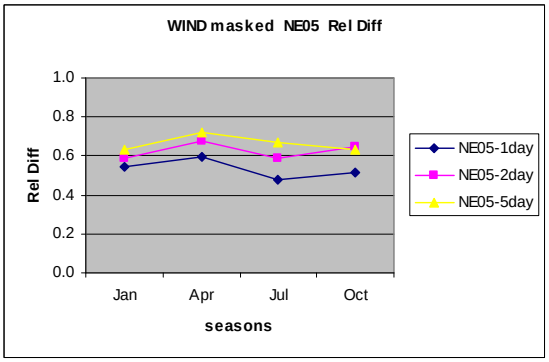

Figure 7 Wind speed Relative error for North east region

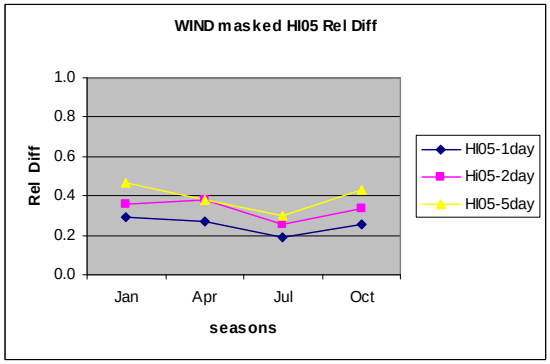

Figure 9 Wind speed Relative error for the Hawaii region

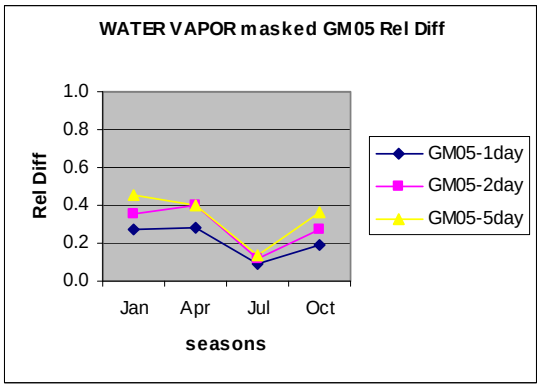

Figure 10 Water Vapor Relative Error for Gulf of Mexico region

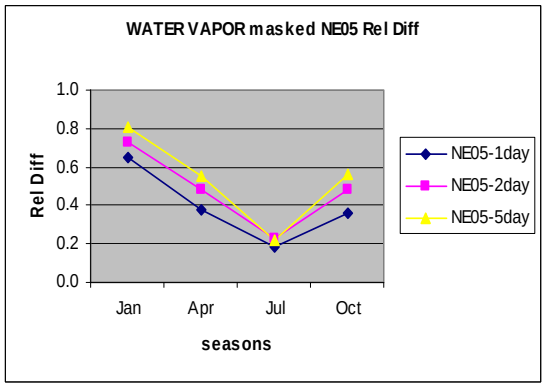

Figure 11 Water Vapor relative errors for the North east region

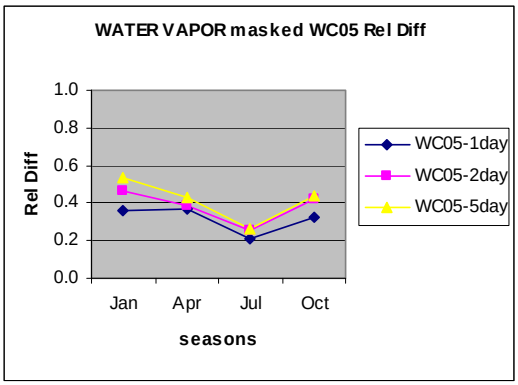

Figure 12 Water Vapor Relative errors for the West Coast region

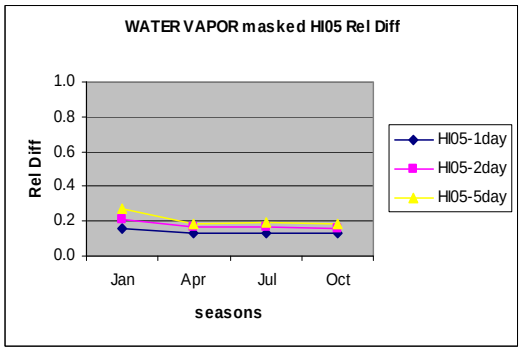

Figure 13 Water Vapor relative errors for the Hawaii region

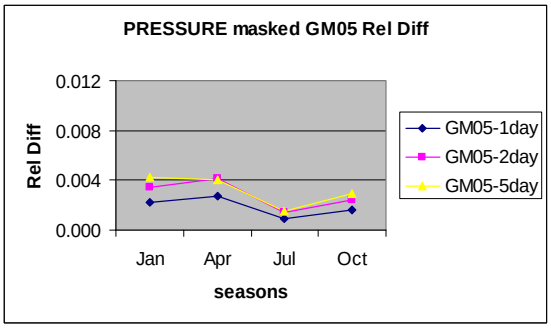

Figure 14 Pressure relative errors for Gulf of Mexico region

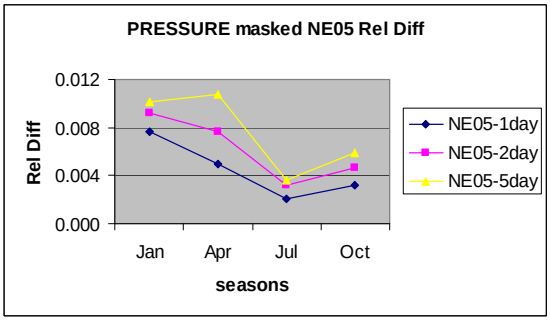

Figure 15 Pressure Relative errors for the North east region

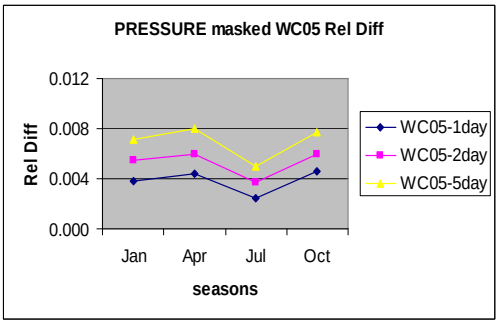

Figure 16 Pressure relative errors for the West Coast region

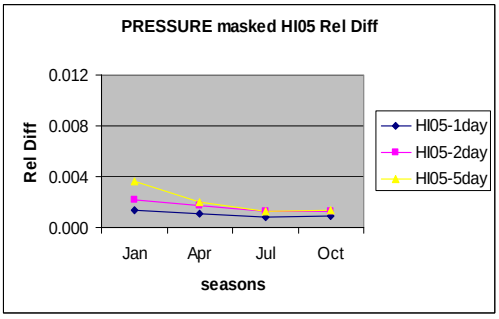

Figure 17 Pressure relative errors for the Hawaii region

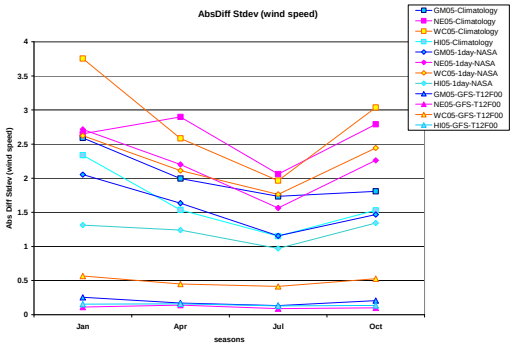

Figure 18 the stdev of wind speed differences in the Ancillary data

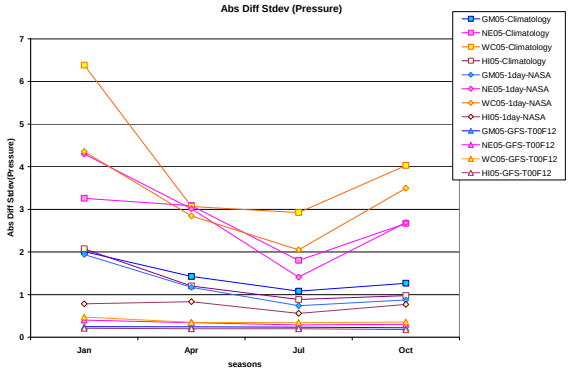

Figure 19 Stdev of Atmospheric pressure differences in the various Ancillary data (GFS and NASA)

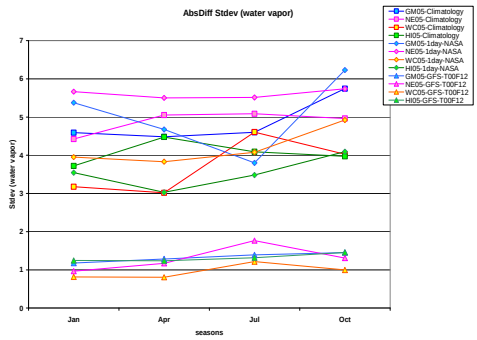

Figure 20 Stdev of the differences in Water Vapor

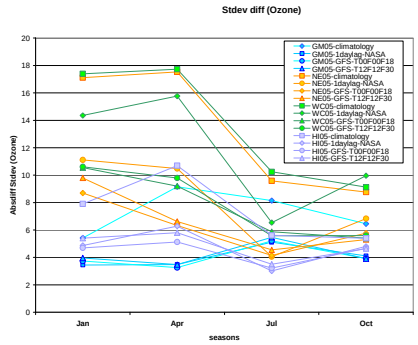

Figure 21 Stdev of the differences in Ozone values retrieved from GFS model forecast and NASA TOAST

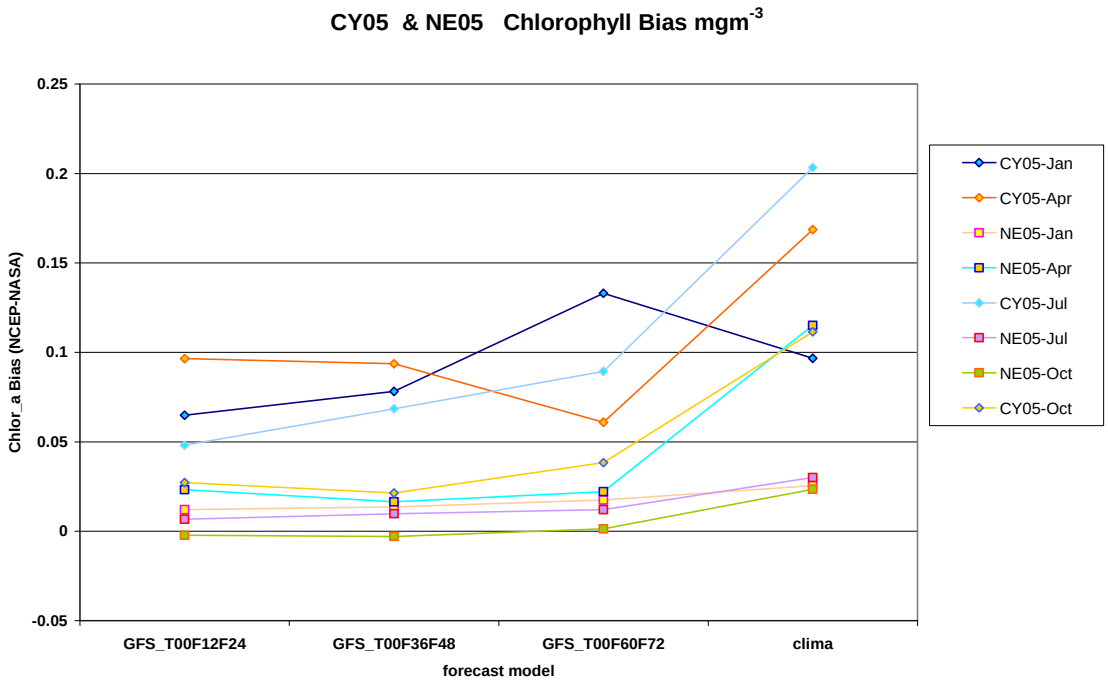

Figure 22 Bias of Chlorophyll product when compared with the NASA science quality stream. Climatology derived values are also shown in the same plot.

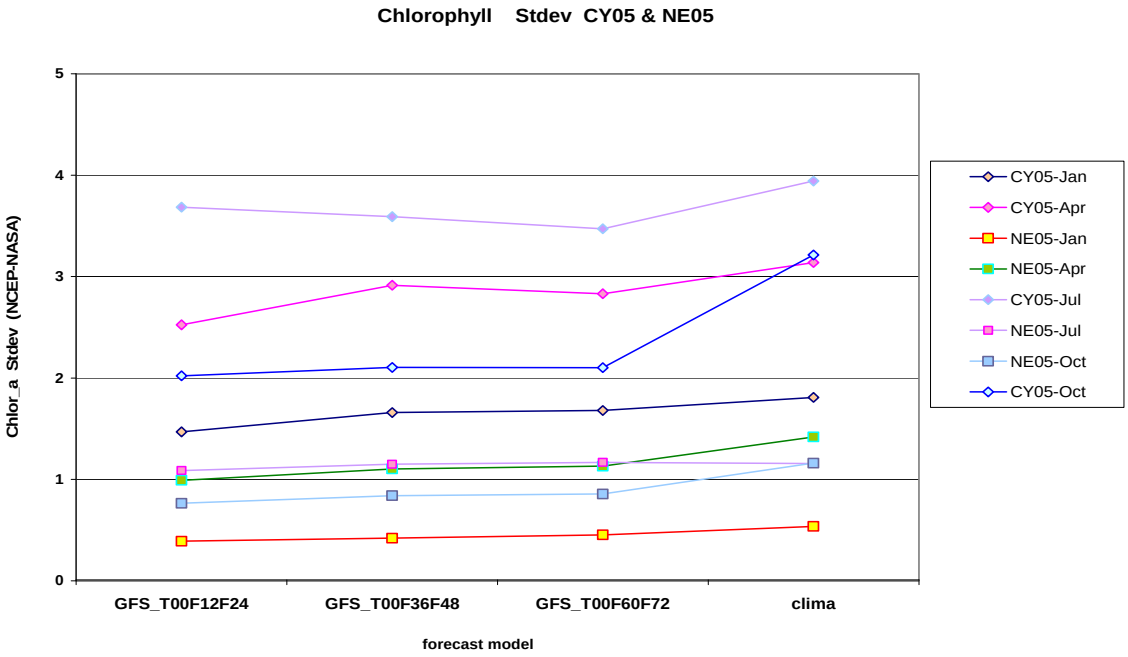

Figure 23 Standard Deviation of the difference is shown for various seasons along with that for the climatology product

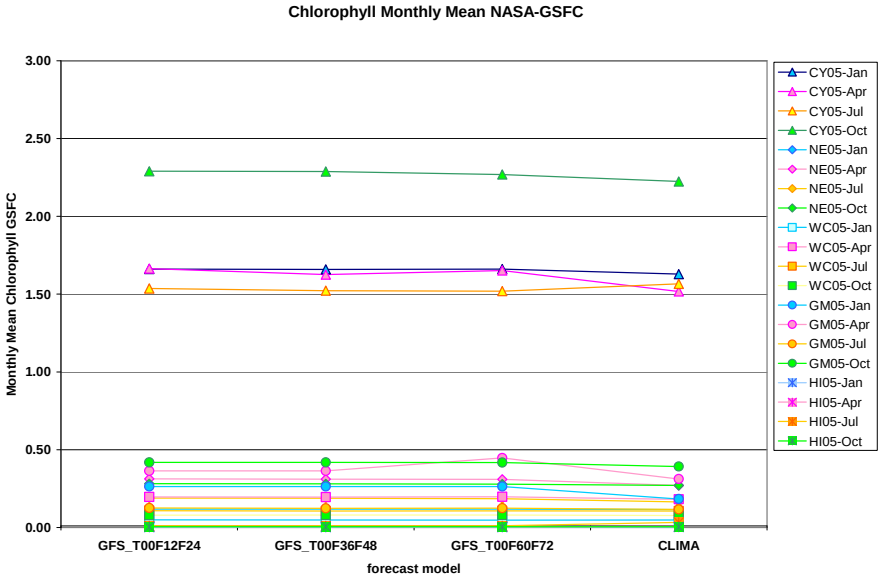

Figure 24 Chlorophyll mean values for the different regions

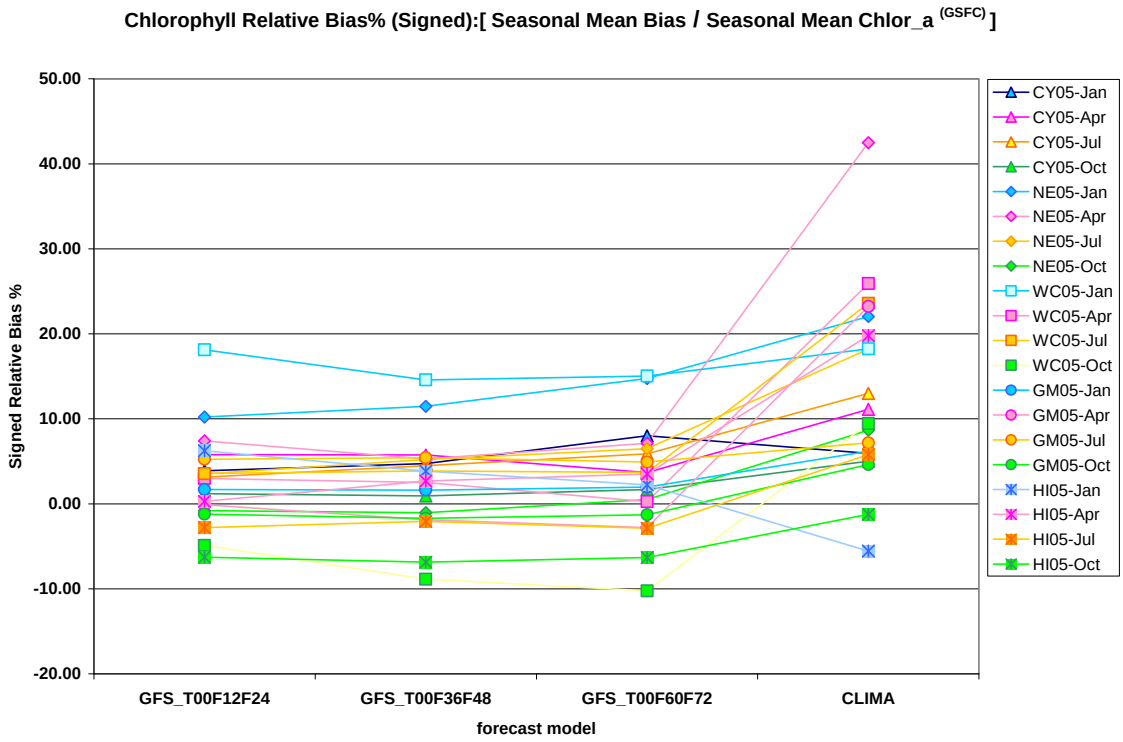

Figure 25 Fractional difference or relative error is shown for the three model forecast data and climatology processed Chlorophyll product.

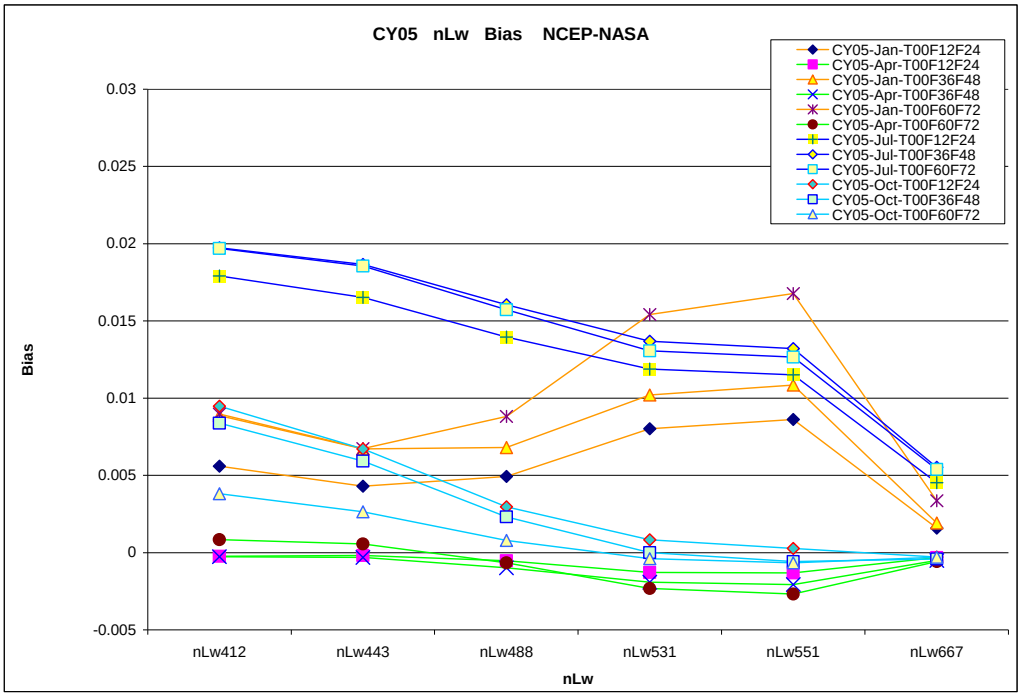

Figure 26 Bias of nLw for CY05 region

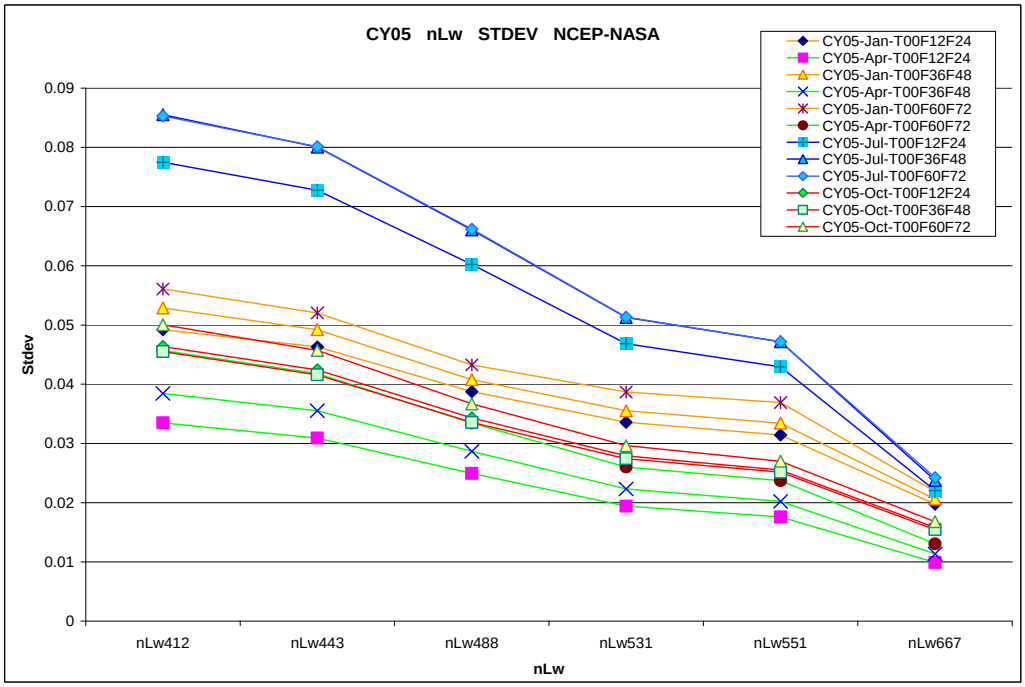

Figure 27 Standard deviation of nLw for CY05 region

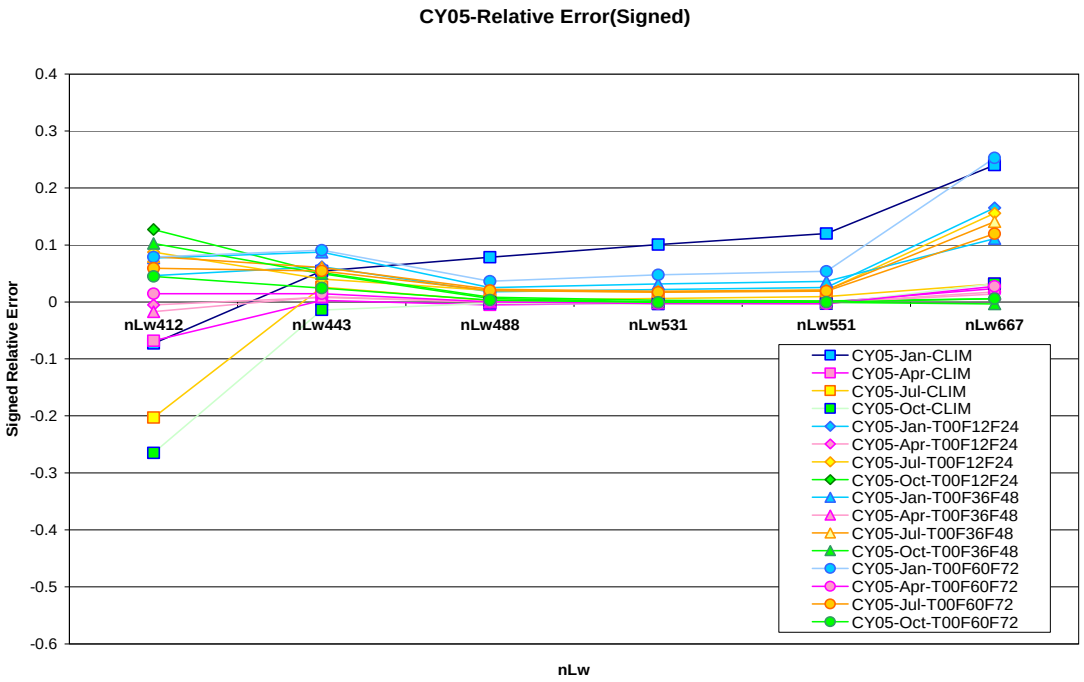

Figure 28 Relative Error of nLws for CY05 region

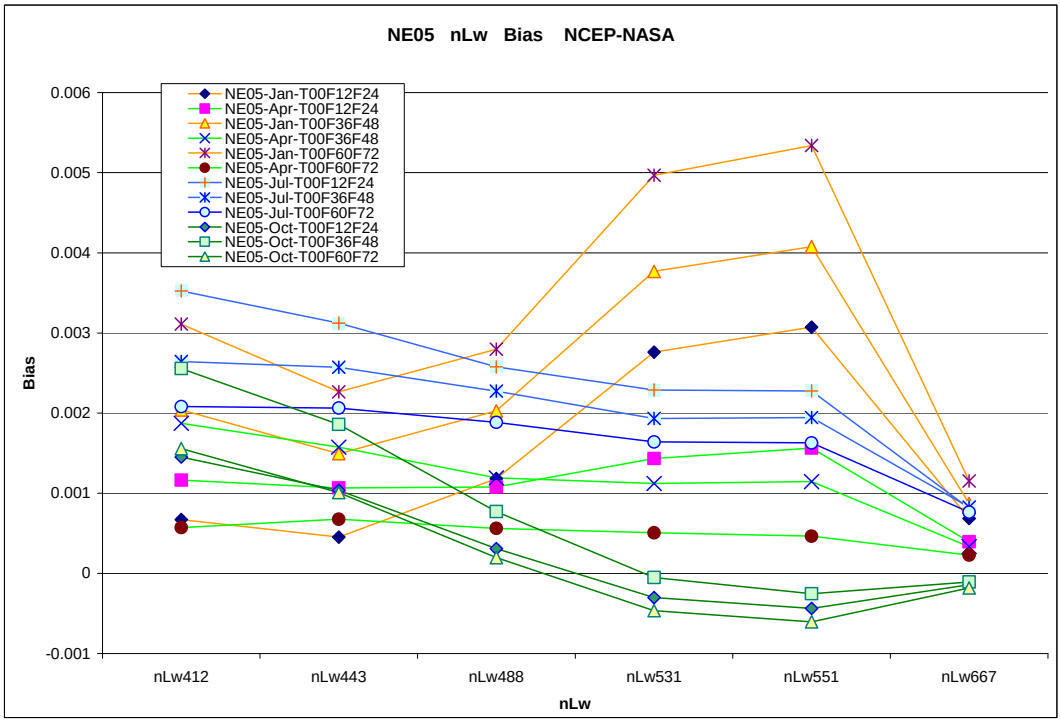

Figure 29 Bias of nLw values for NE05

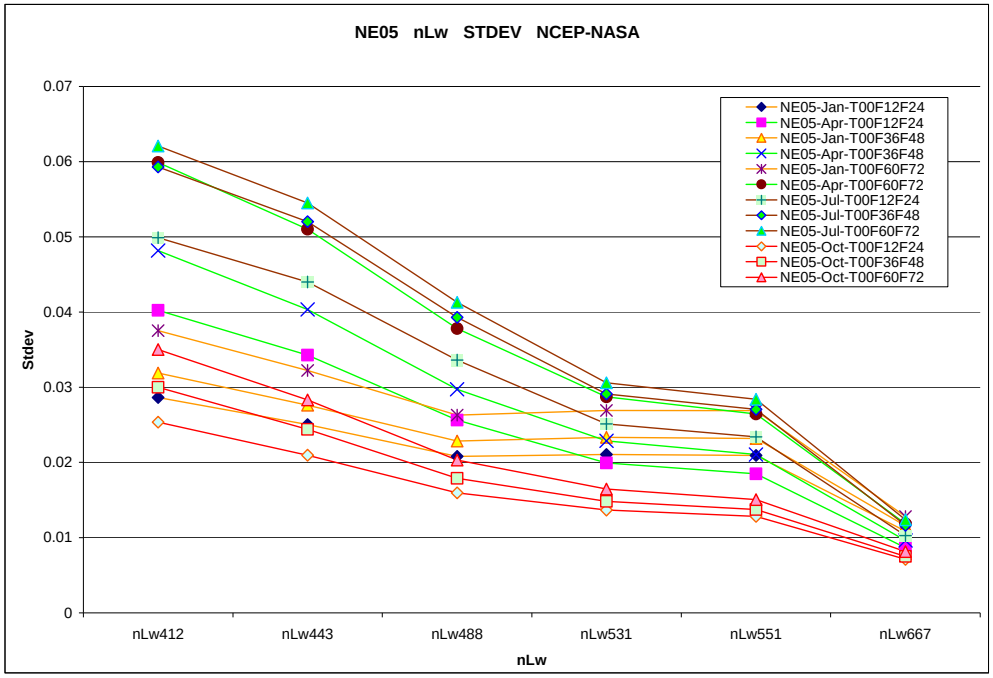

Figure 30 Standard deviation of nLw derived values for NE

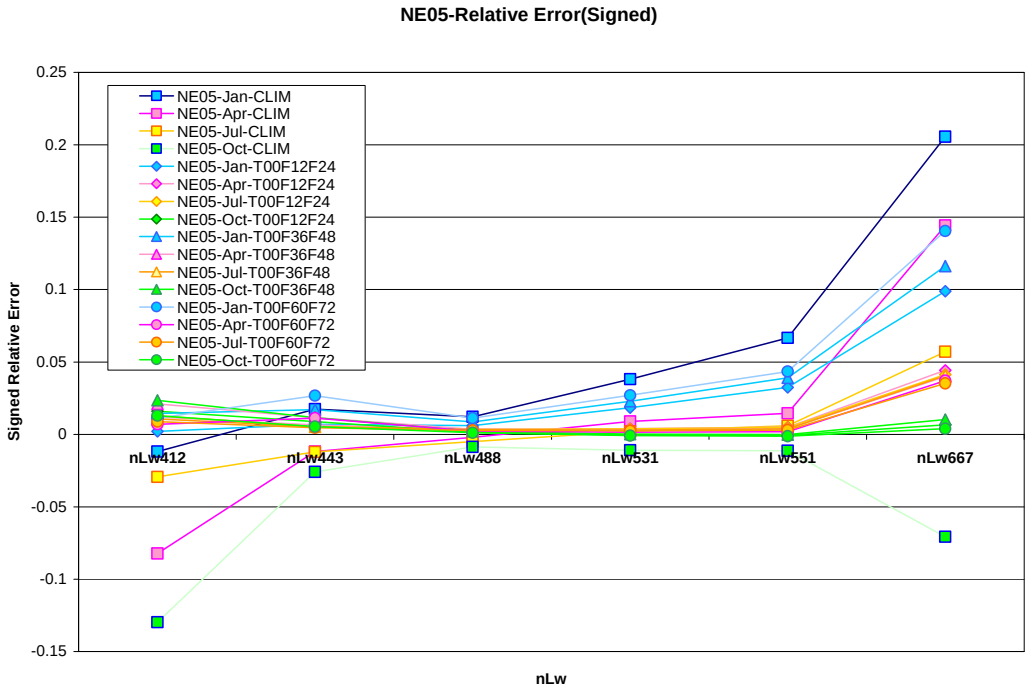

Figure 31 Signed Relative Differences for NE

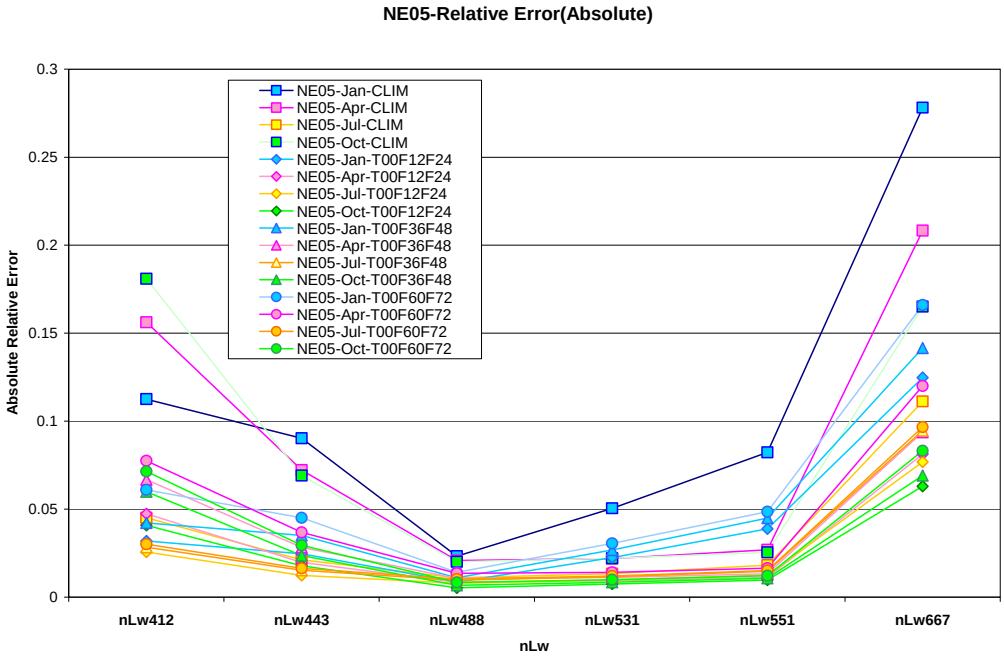

Figure 32 Absolute Relative Errors for NE05

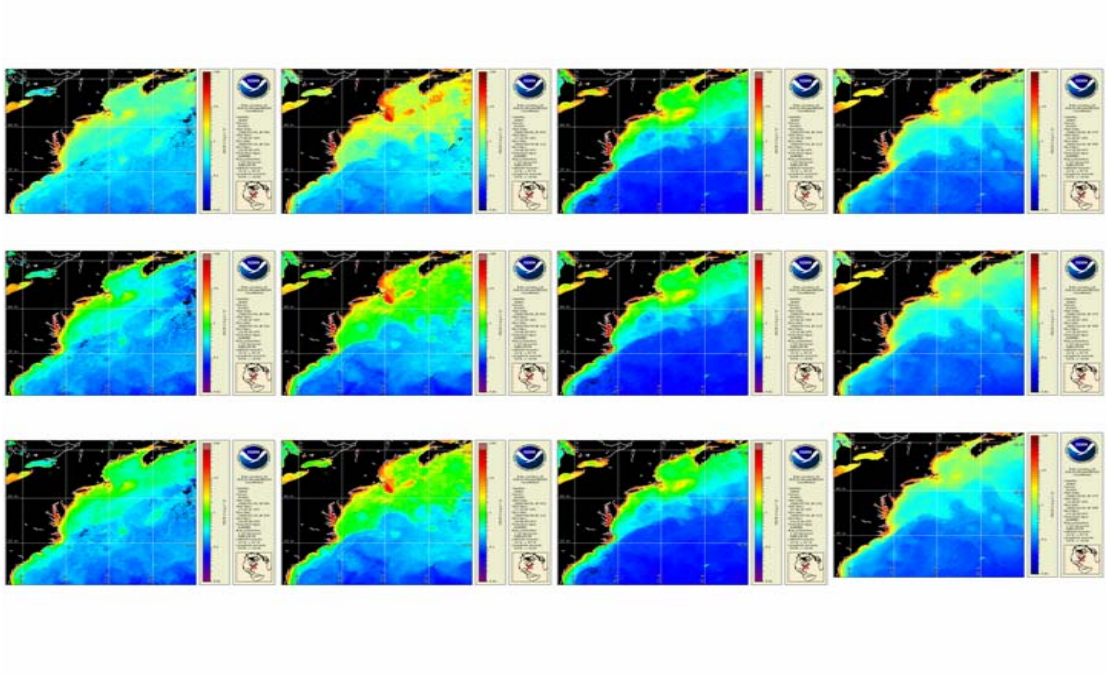

Figure 33 Chlorophyll concentrations for the Northeast region are shown here for the four seasons, same as in the previous figure. The bottom row is for NCEP-GFS model data used as Ancillary for processing.

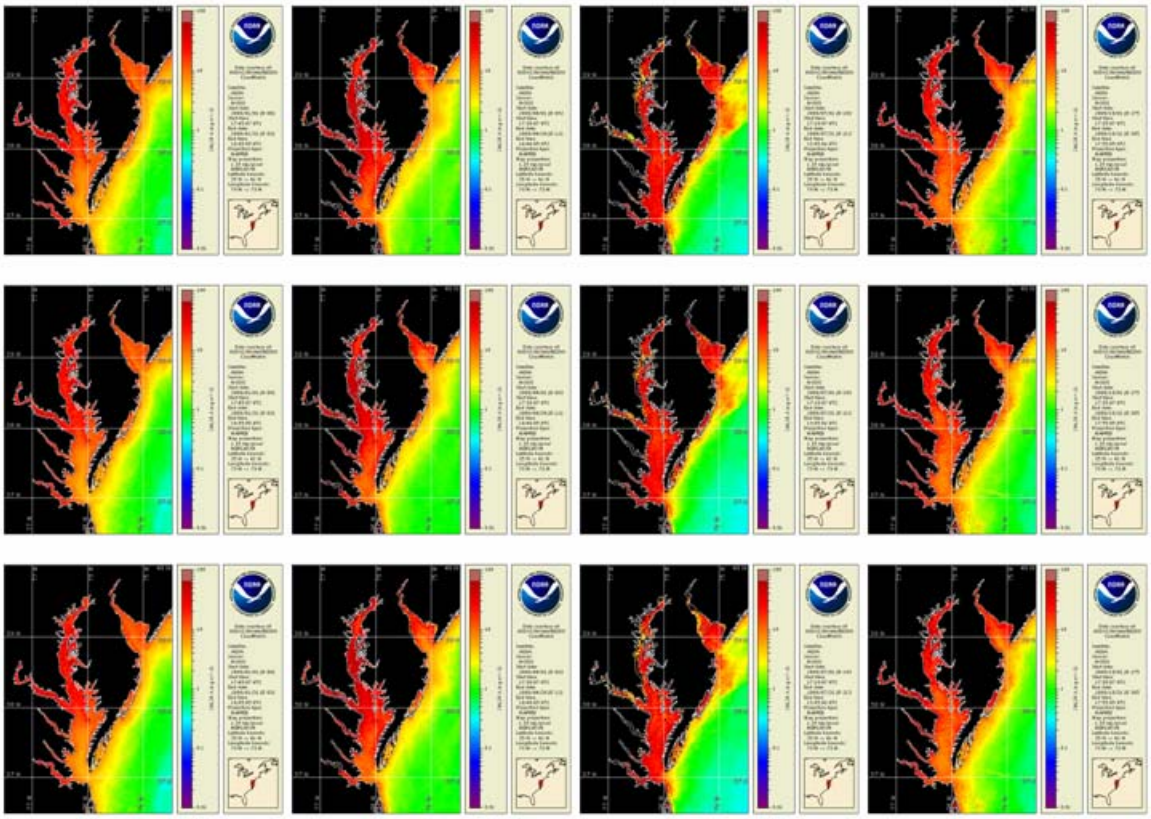

Figure 34 Chlorophyll concentration images for the four seasons Jan, Apr, Jul & Oct (Left-to-Right). Top row: Climatology for Ancillary data, Middle: NASA science quality Ancillary used, Last row: NCEP-GFS Ancillary used.

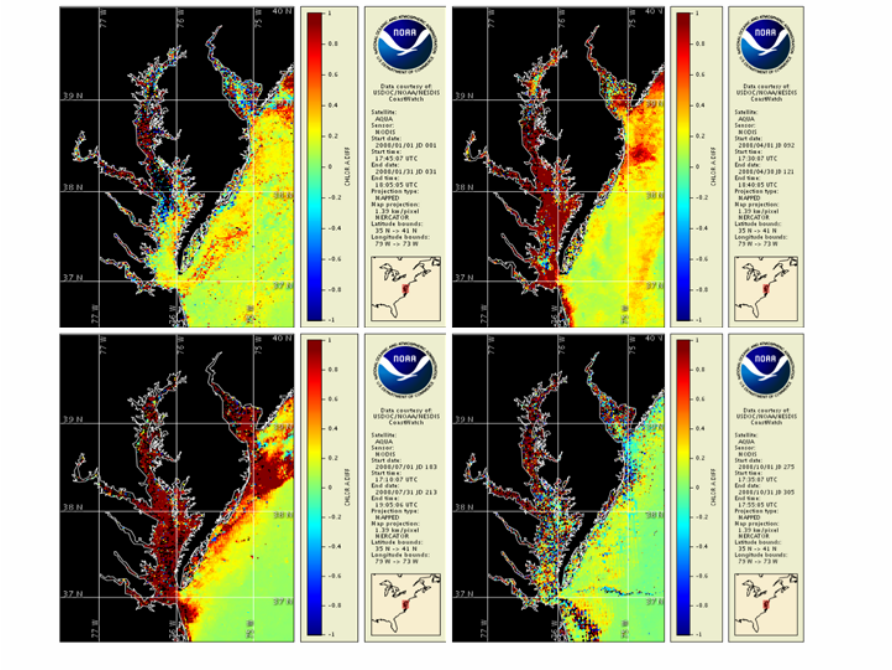

Figure 35 Climatology processed differences in Chlorophyll for all four seasons (Jan-Apr-Jul-Oct) in clockwise arrangement. The range is [-1.0, 1.0] in Chlorophyll units of mg m^{-3}.

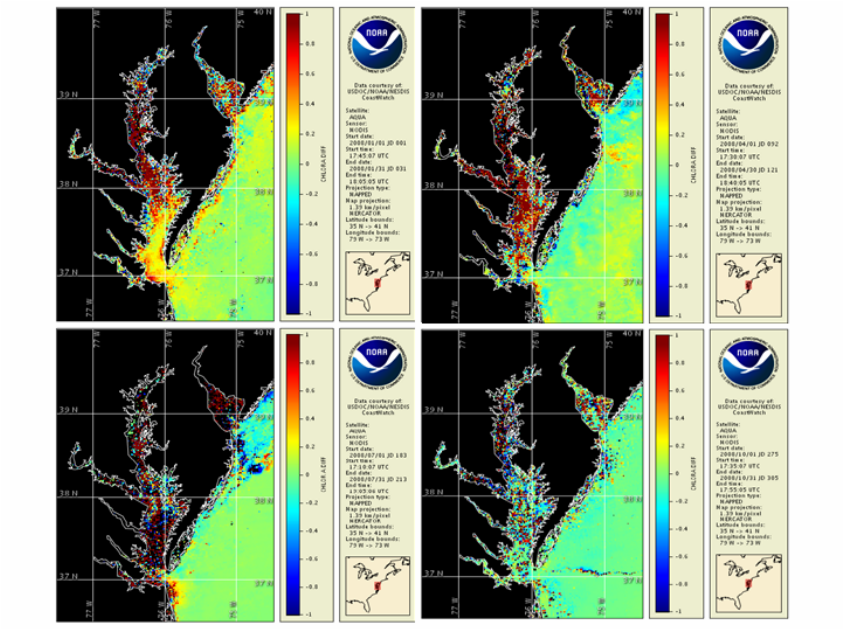

Figure 36 NCEP GFS T00F18F30 forecast processed Chlorophyll differences for the four seasons.

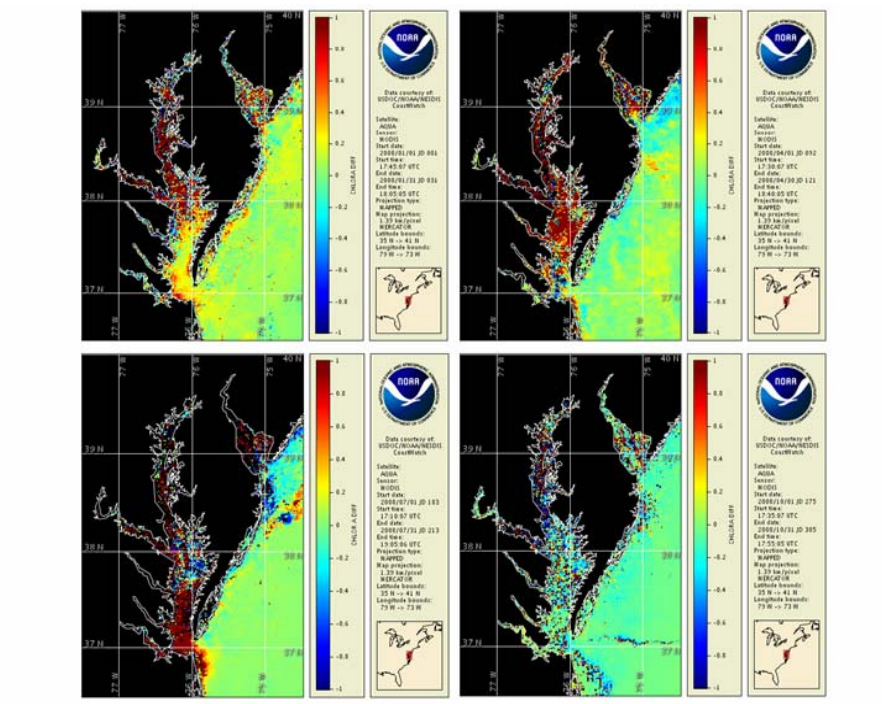

Figure 37 NCEP GFS T00F42F54 forecast processed Chlorophyll differences for the four seasons, same as above.

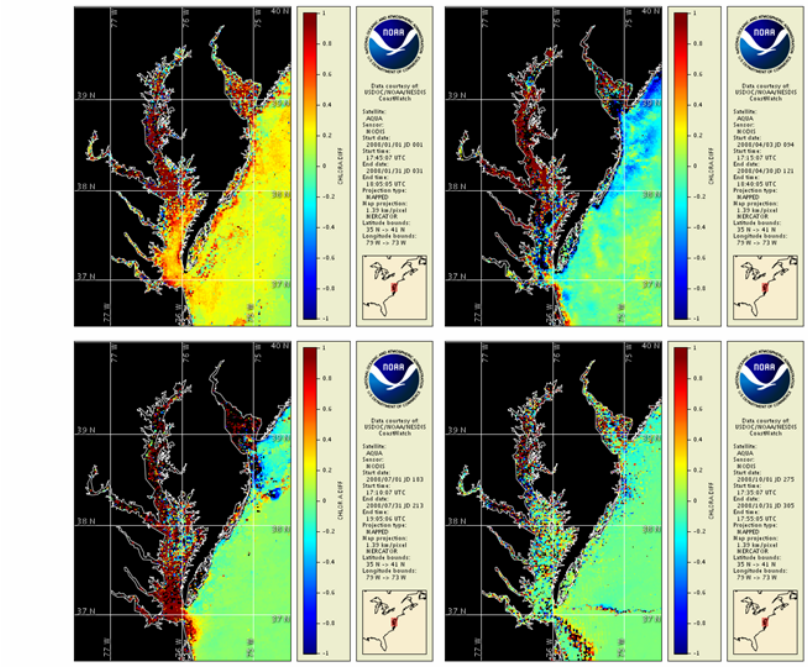

Figure 38 NCEP GFS T00F66F78 forecast processed Chlorophyll differences for the same seasons shown in previous figures

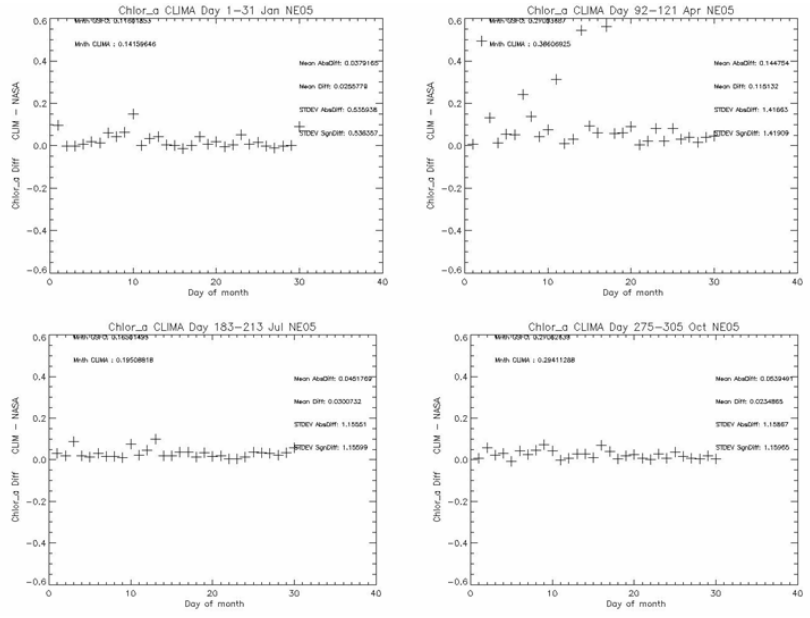

Figure 39 Time series of the mean value of Chlorophyll differences when using Climatology for Ancillary datasets. The y-axis range is [-0.6, 0.6]

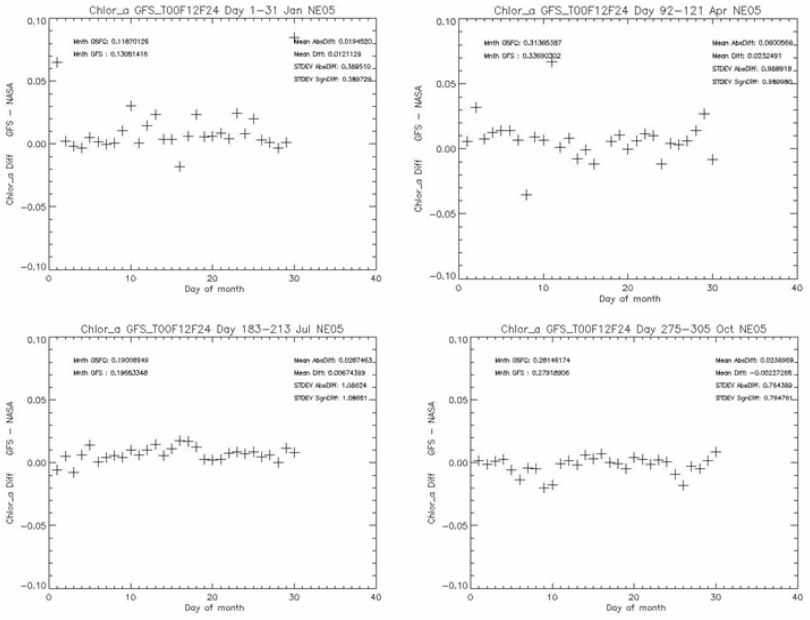

Figure 40 Time series of the mean Chlorophyll differences calculated for all the valid pixels of final product, when using GFS NCEP Ancillary compared with when using the NASA Ancillary dataset for the North east region for all four seasons.

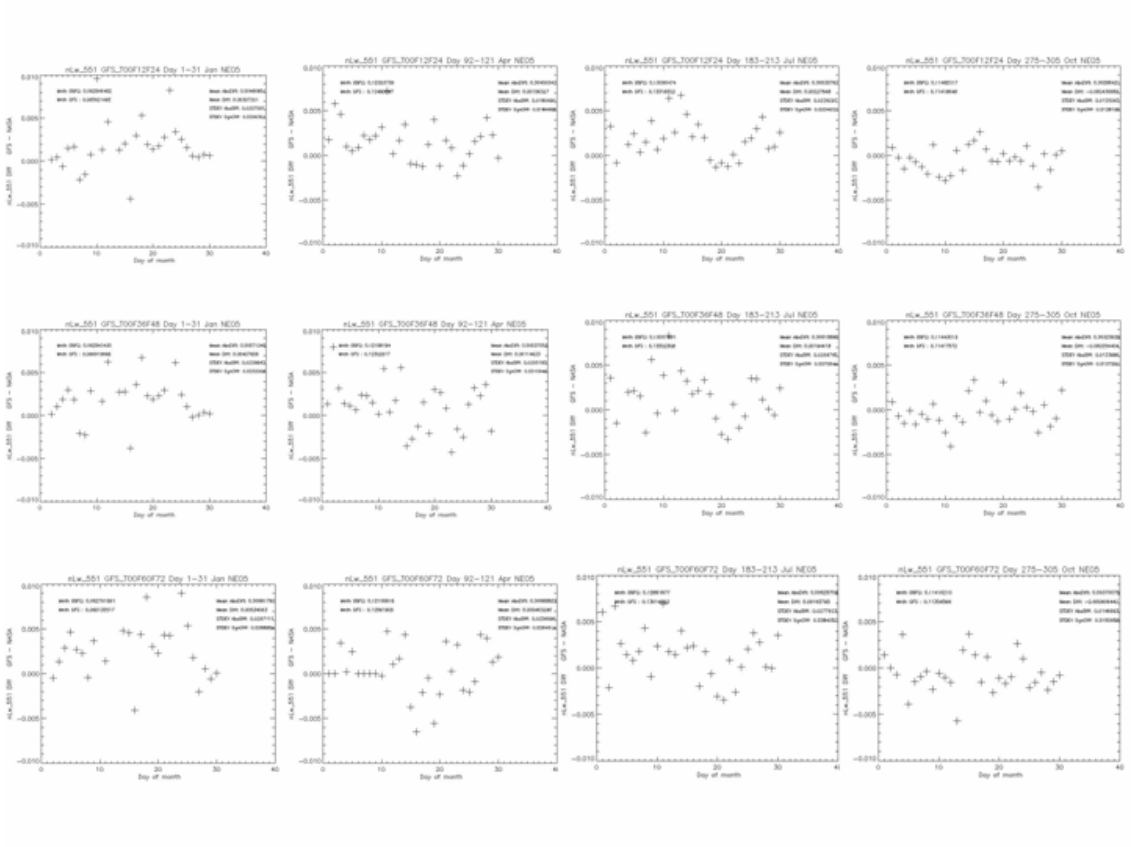

Figure 41 Time series of the differences for nLw551 values for the four seasons Jan, Apr, Jul, Oct (columns) and three increasing forecast lag (rows) from T00F12F24, T00F36F48 to T00F60F72.

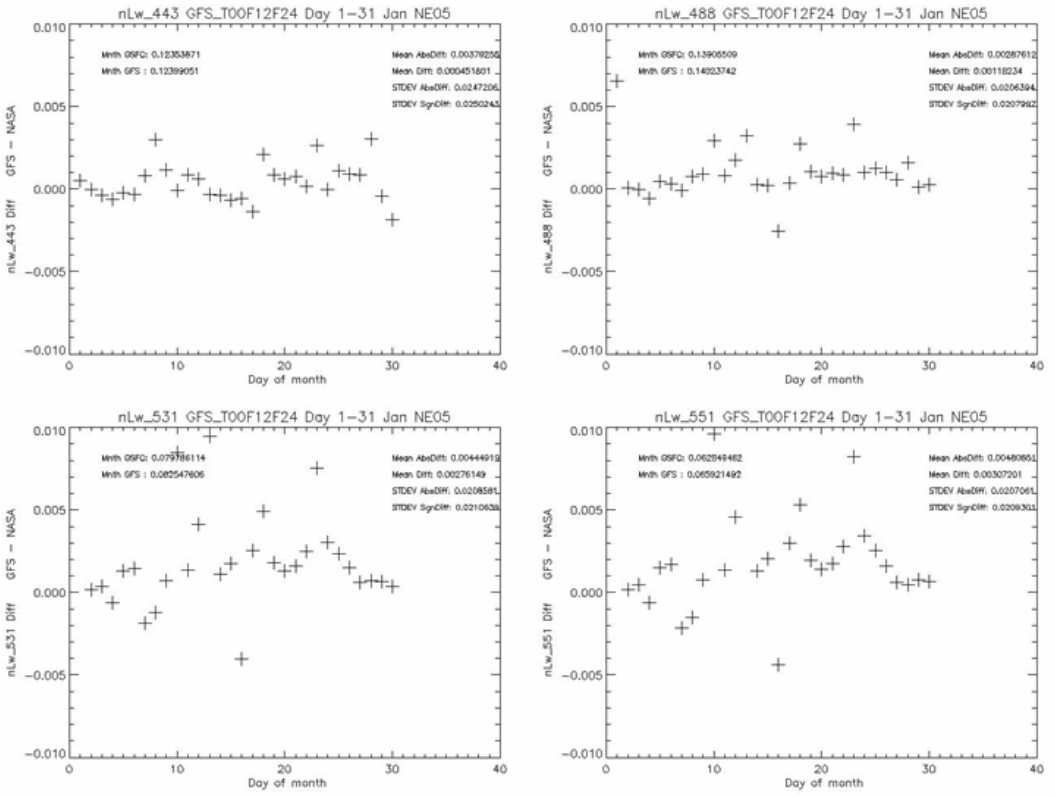

Figure 42 Time series of the mean differences for nLws 443,488,531,551 nm for the month of January using T00F12F24 GFS forecast

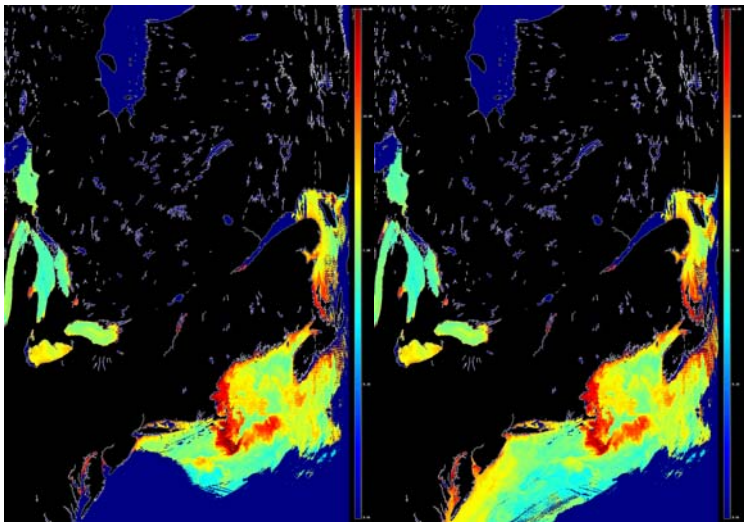

Figure 43 Day 106 MODIS data granule processed using Climatology for Ancillary on the left and NCEP GFS Ancillary on the right. The left image has many more pixels masked out

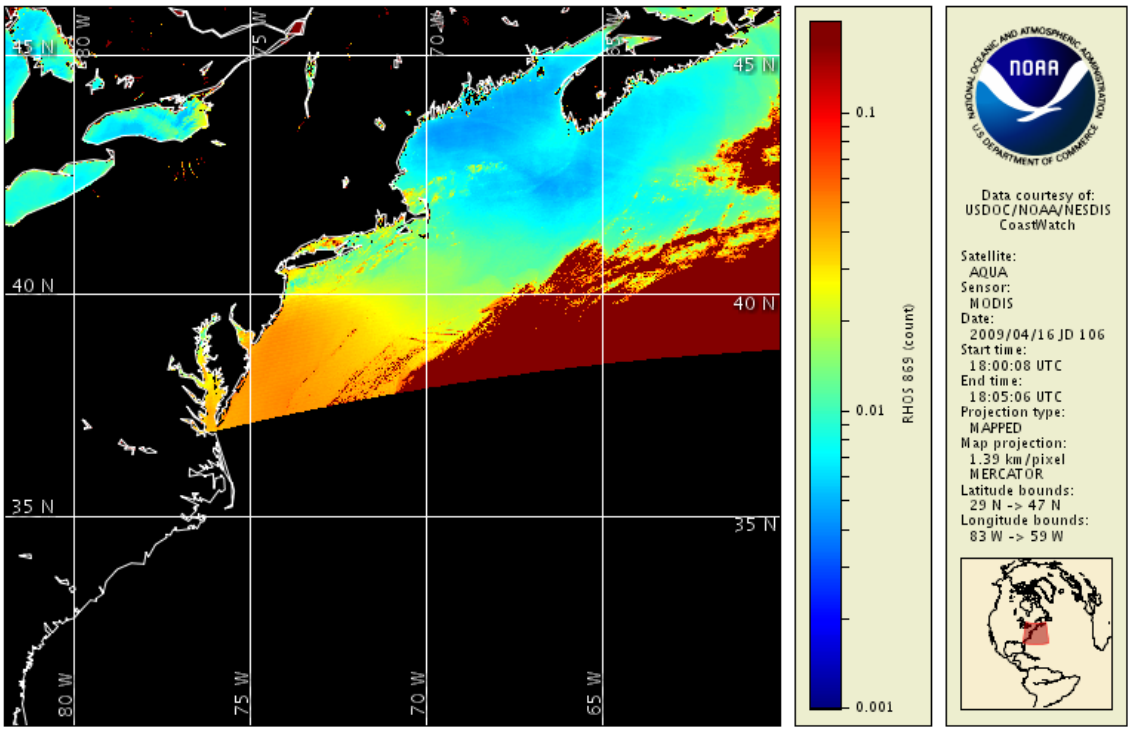

Figure 44 Day 106, 2009 rhos_869 image shows the region where pixels are getting masked close to the threshold value of 0.027 used in the cloud mask algorithm.

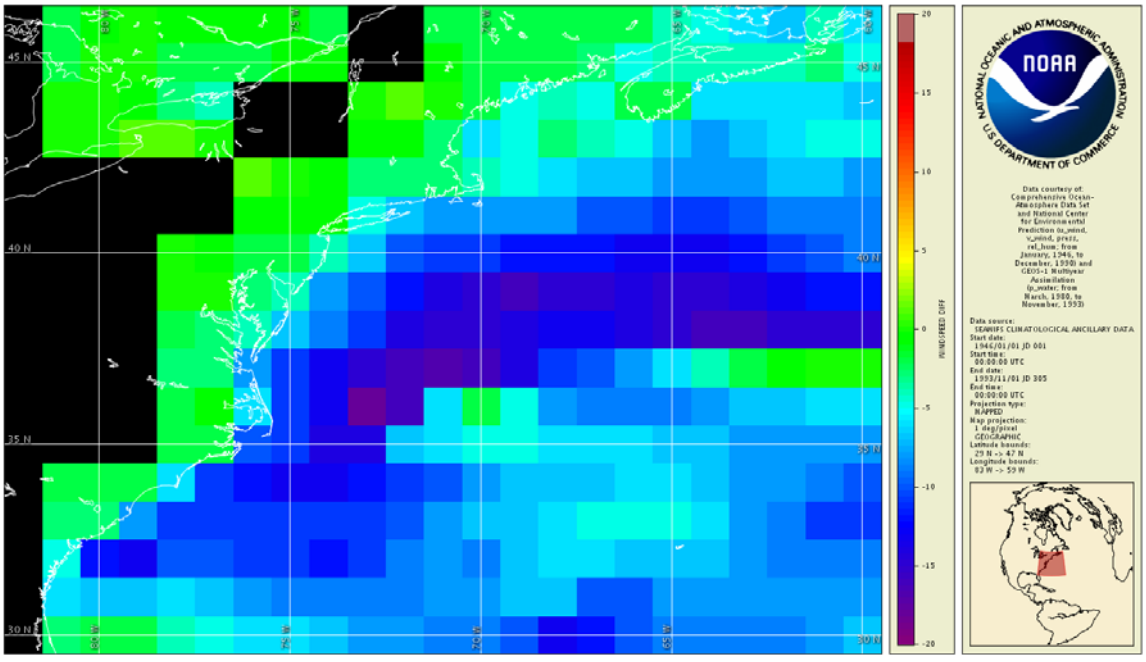

Figure 45 Wind speed difference (CLIMA - OBPG) for day 106, 2009.

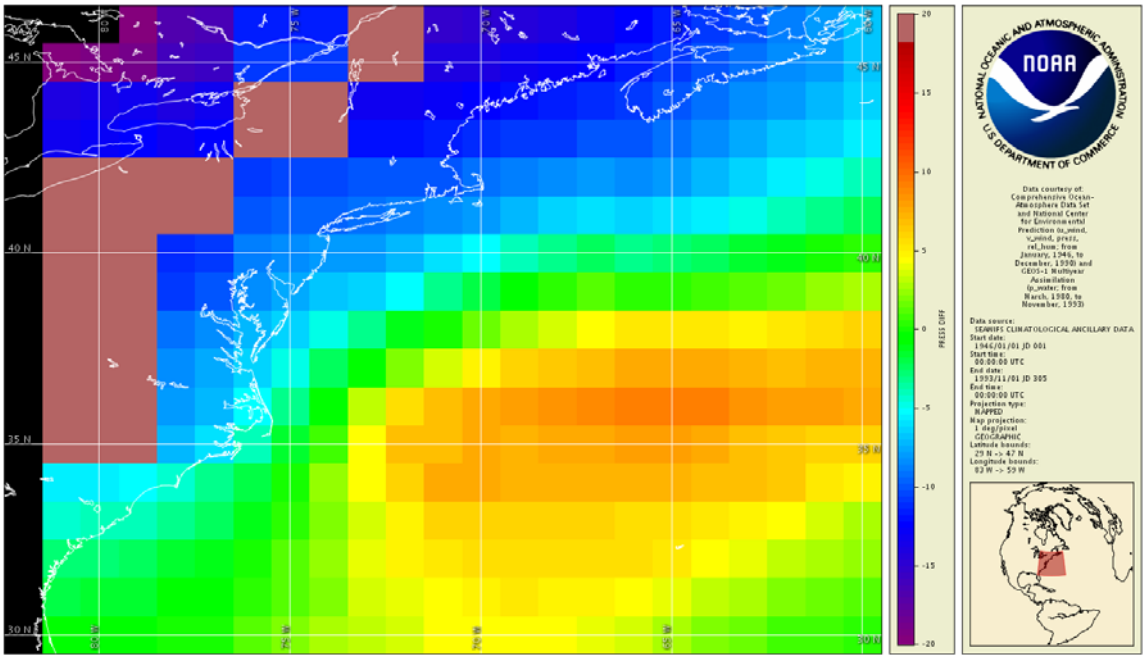

Figure 46 Pressure difference (CLIMA - OBPG) for day 106, 2009.

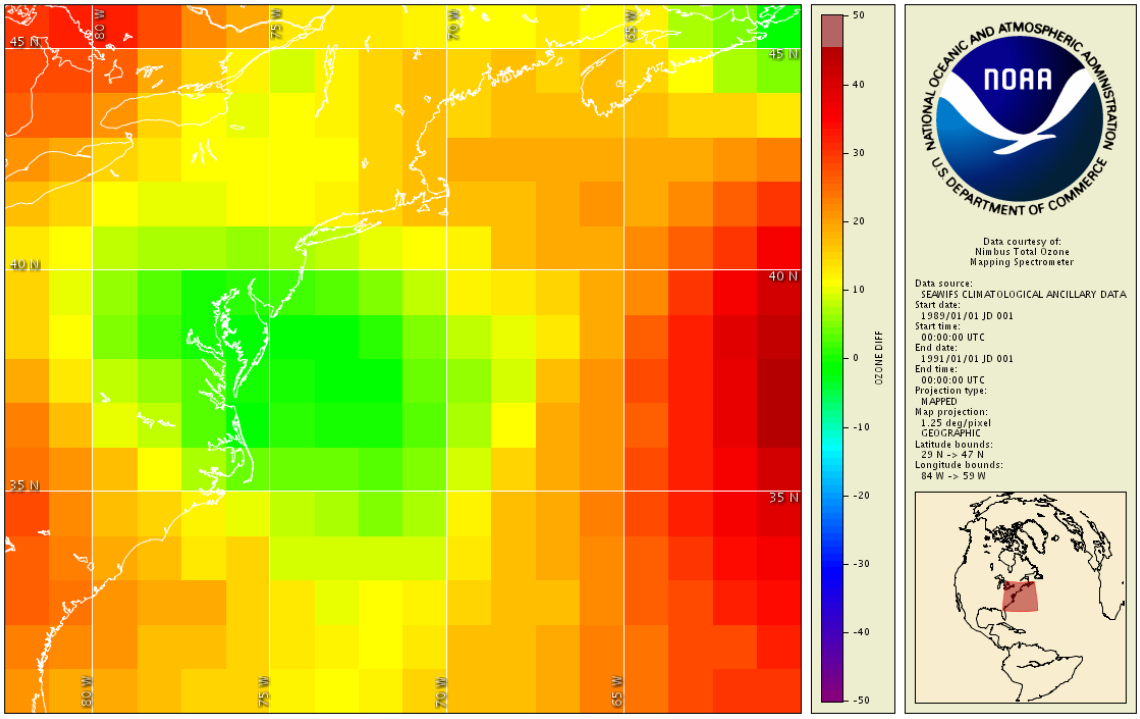

Figure 47 Ozone difference (Clima - OBPG) for day 106, 2009.

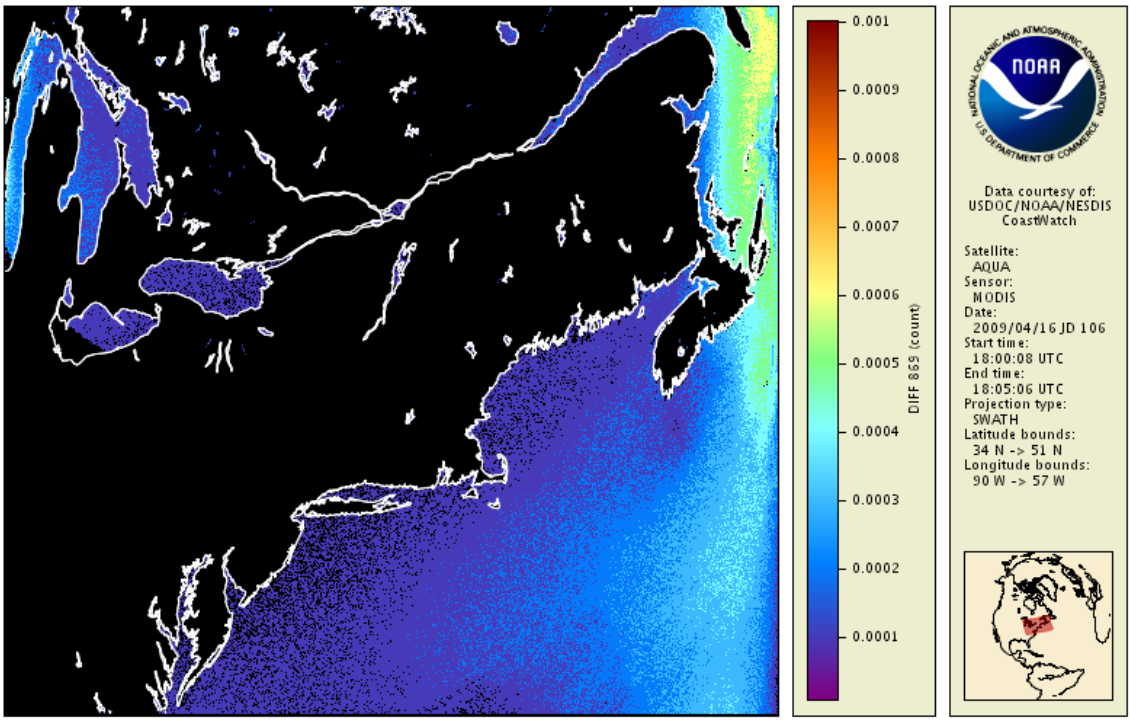

Figure 48 Difference in the rho_869 values between Climatology and NASA is shown. There is no apparent pattern which matches the cloud masks seen in the climatology product. (ref fig 44)

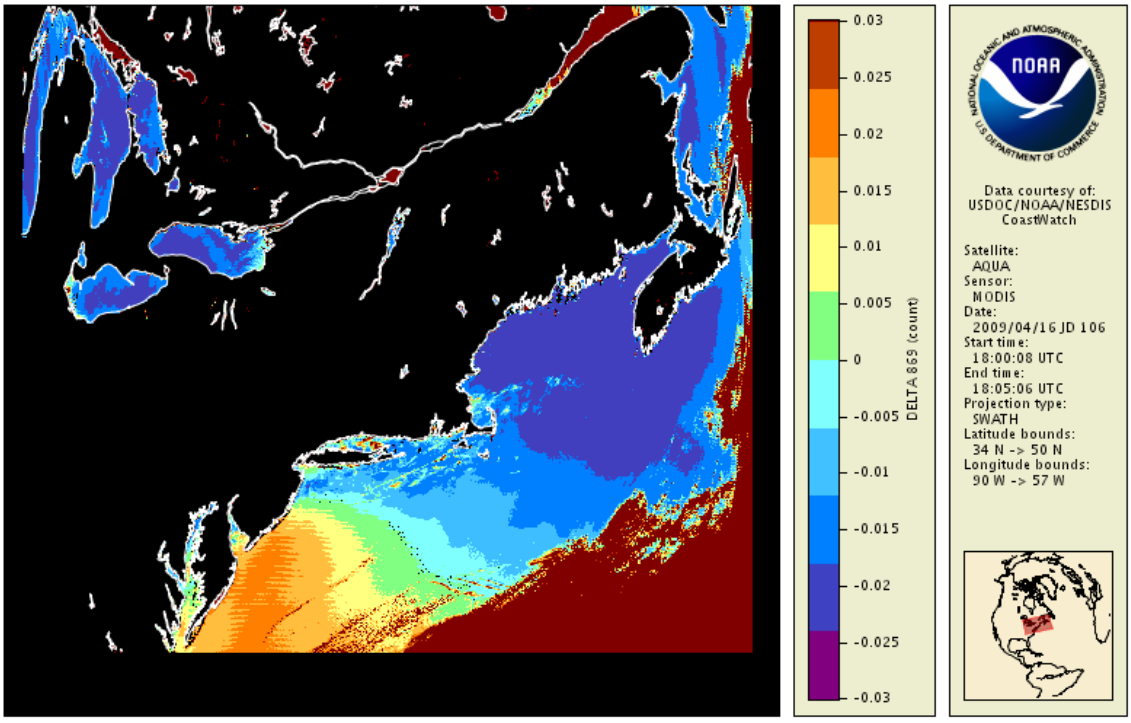

Figure 49 delta rho_869: rho_869 - 0.027. This shows the regions where the reflectance is above the threshold value for cloud flagging. All values above zero will be flagged as cloud.

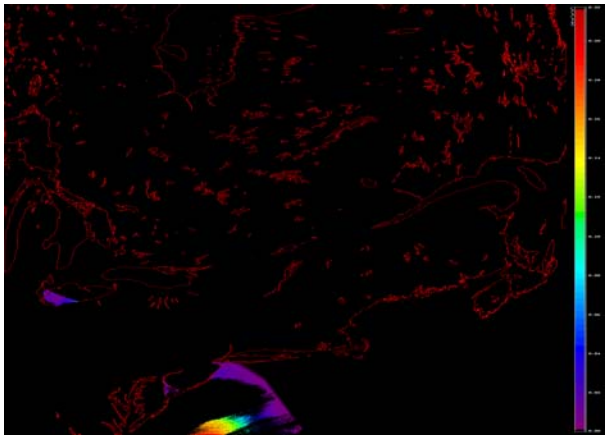

Figure 50 Sun glint radiance tLg_869 when using Climatology for ancillary data

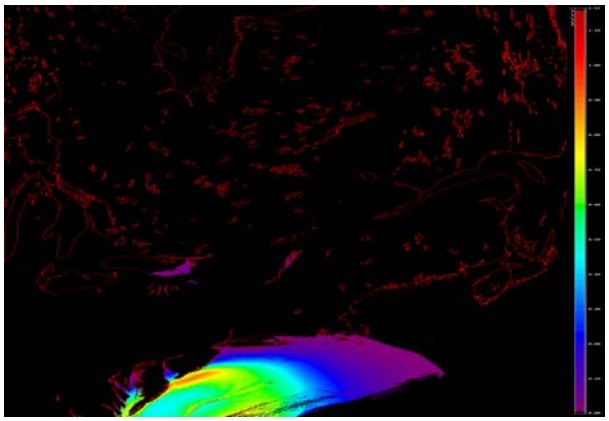

Figure 51 Sun glint radiance tLg_869 when using NASA definitive Ancillary data

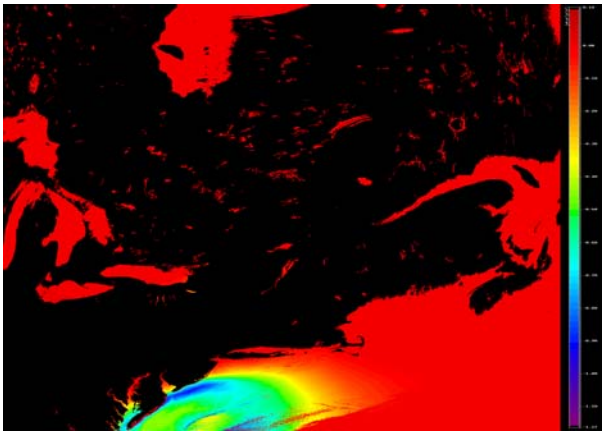

Figure 52 Difference tLg_869: Clima – NASA. This shows for coastal area the glint correction is higher when using NASA ancillary with higher wind speed values compared to Climatology.

References:

1. Kalnay, E. : Atmospheric Modeling, Data Assimilation and Predictability

2. Buizza, R., Petroliagis, T., Palmer, T. N., Barkmeijer, J., Hamrud, M., Hollingsworth, A., Simmons, A., and Wedi, N., 1998: Impact of model resolution and ensemble size on the performance of an ensemble prediction system. Q. J. R. Meteorol. Soc., 124, 1935-1960.

3. Houtekamer, P. L., and H. L. Mitchell, 1998: Data assimilation using an ensemble Kalman filter technique. Mon. Wea. Rev., 126, 796-811.

4. Toth, Z., and E. Kalnay, 1993: Ensemble Forecasting at the NMC: The generation of perturbations. Bull. Amer. Meteorol. Soc., 74, 2317-2330.

5. Toth, Z., and E. Kalnay, 1997: Ensemble forecasting at NCEP and the breeding method. Mon. Wea. Rev, 125, 3297-3319.

6. Kanamitsu, M., 1989: Description of the NMC global data assimilation and forecast system. Wea. and Forecasting, 4, 335-342.

7. Kalnay, E. and M. Kanamitsu, 1988: Time Scheme for Strongly Nonlinear Damping Equations. Mon. Wea. Rev., 116, 1945-1958.

8. Kalnay, M. Kanamitsu, and W.E. Baker, 1990: Global numerical weather prediction at the National Meteorological Center. Bull. Amer. Meteor. Soc., 71, 1410-1428.

9. Kanamitsu, M., J.C. Alpert, K.A. Campana, P.M. Caplan, D.G. Deaven, M. Iredell, B. Katz, H.-L. Pan, J. Sela, and G.H. White, 1991: Recent changes implemented into the global forecast system at NMC. Wea. and Forecasting, 6, 425-435.

10. Sela, J. G., 1980: Spectral modeling at NMC, *Mon. Wea. Rev.*, pp. 1279-1292.

11. Sela, J. G., 1982: The NMC spectral model, *NOAA Technical Report NWS 30*, 36 pp.

12. Toth, Z., and I. Szunyogh, 1997: Review of the use of ECMWF ensemble data for targeting upstream observations during the FASTEX field experiments. In: Proceedings of the FASTEX Upstream Observations Workshop, NCEP, Camp Springs, Md, April 10-11, 1997. NOAA/NWS/NCEP Office Note 420, p. 131. [Available from: Environmental Modeling Center, 5200 Auth Rd., WWB, Rm. 207, Camp Springs, MD 20746.]

13. Alpert, J.C., S-Y Hong and Y-J Kim, 199x: Sensitivity of cyclogenesis to lower troposphere enhancement of gravity wave drag using the Environmental Modeling Center medium range model. REF

14. Alpert, J.C., M. Kanamitsu, P.M. Caplan, J.G. Sela, G.H. White, and E. Kalnay, 1988: Mountain induced gravity wave drag parameterization in the NMC medium-range model. Preprints of the Eighth Conference on Numerical Weather Prediction, Baltimore, MD, American Meteorological Society, 726-733.

15. Arakawa, A. and W. H. Shubert, 1974: Interaction of a Cumulus Ensemble with the Large-Scale Environment, Part I. J. Atmos. Sci., 31, 674-704.

16. Asselin, R., 1972: Frequency filter for time integrations. Mon. Wea. Rev., 100, 487-490.

17. Betts, A.K., S.-Y. Hong and H.-L. Pan, 1996: Comparison of NCEP-NCAR Reanalysis with 1987 FIFE data. Mon. Wea. Rev., 124, 1480-1498

18. Briegleb, B. P., P. Minnus, V. Ramanathan, and E. Harrison, 1986: Comparison of regional clear-sky albedo inferred from satellite observations and model computations. J. Clim. and Appl. Meteo., 25, 214-226.

19. Campana, K. A., Y-T Hou, K. E. Mitchell, S-K Yang, and R. Cullather, 1994: Improved diagnostic cloud parameterization in NMC's global model. Preprints of the Tenth Conference on Numerical Weather Prediction, Portland, OR, American Meteorological Society, 324-325.

20. Charnock, H., 1955: Wind stress on a water surface. Quart. J. Roy. Meteor. Soc., 81, 639-640.

21. Chen, F., K. Mitchell, J. Schaake, Y. Xue, H.-L. Pan, V. Koren, Q. Y. Duan, M. Ek, and A. Betts, 1996: Modeling of land surface evaporation by four schemes and comparison with FIFE observations. J. Geophys. Res., 101, D3, 7251-7268.

22. Chou, M-D, 1990: Parameterizations for the absorption of solar radiation by O2 and CO2 with application to climate studies. J. Climate, 3, 209-217.

23. Chou, M-D, 1992: A solar radiation model for use in climate studies. J. Atmos. Sci., 49, 762-772.

24. Chou, M-D and K-T Lee, 1996: Parameterizations for the absorption of solar radiation by water vapor and ozone. J. Atmos. Sci., 53, 1204-1208.

25. Chou, M.D., M. J. Suarez, C. H. Ho, M. M. H. Yan, and K. T. Lee, 1998: Parameterizations for cloud overlapping and shortwave single scattering

properties for use in general circulation and cloud ensemble models. J. Climate, 11, 202- 214.

26. Clough, S.A., M.J. Iacono, and J.-L. Moncet, 1992: Line-by-line calculations of atmospheric fluxes and cooling rates: Application to water vapor. J. Geophys. Res., 97, 15761-15785.

27. Coakley, J. A., R. D. Cess, and F. B. Yurevich, 1983: The effect of tropospheric aerosols on the earth's radiation budget: a parameterization for climate models. J. Atmos. Sci., 42, 1408-1429.

28. Dorman, J.L., and P.J. Sellers, 1989: A global climatology of albedo, roughness length and stomatal resistance for atmospheric general circulation models as represented by the Simple Biosphere model (SiB). J. Appl. Meteor., 28, 833-855.

29. Ebert, E.E., and J.A. Curry, 1992: A parameterization of ice cloud optical properties for climate models. J. Geophys. Res., 97, 3831-3836.

30. Frohlich, C. and G. E. Shaw, 1980: New determination of Rayleigh scattering in the terrestrial atmosphere. Appl. Opt., 14, 1773-1775.

31. Fu, Q., 1996: An accurate parameterization of the solar radiative properties of cirrus clouds for climate models. J. Climate, 9, 2058-2082.

32. Hess, M., P. Koepke, and I. Schult, 1998: Optical properties of aerosols and clouds: The software package OPAC. Bull. Am. Meteor. Soc., 79, 831-844.

33. Grell, G. A., 1993: Prognostic Evaluation of Assumprions Used by Cumulus Parameterizations. Mon. Wea. Rev., 121, 764-787.

34. Grumbine, R. W., 1994: A sea-ice albedo experiment with the NMC medium range forecast model. Weather and Forecasting, 9, 453-456.

35. Hong, S.-Y. and H.-L. Pan, 1996: Nonlocal boundary layer vertical diffusion in a medium-range forecast model. Mon. Wea. Rev., 124, 2322-2339.

36. Hong, S.-Y., 1999: New global orography data sets. NCEP Office Note #424.

37. Hou, Y-T, K. A. Campana and S-K Yang, 1996: Shortwave radiation calculations in the NCEP's global model. International Radiation Symposium, IRS-96, August 19-24, Fairbanks, AL.

38. Hou, Y.-T., S. Moorthi, and K.A. Campana, 2002: Parameterization of solar radiation transfer in the NCEP models. NCEP Office Note 441.

39. Hu, Y.X., and K. Stamnes, 1993: An accurate parameterization of the radiative properties of water clouds suitable for use in climate models. J. Climate, 6, 728-742.

40. Joseph, D., 1980: Navy 10' global elevation values. National Center for Atmospheric Research notes on the FNWC terrain data set, 3 pp.

41. Kalnay, E. and M. Kanamitsu, 1988: Time Scheme for Stronglyt Nonlinear Damping Equations. Mon. Wea. Rev., 116, 1945-1958.

42. Kalnay, M. Kanamitsu, and W.E. Baker, 1990: Global numerical weather prediction at the National Meteorological Center. Bull. Amer. Meteor. Soc., 71, 1410-1428.

43. Kanamitsu, M., 1989: Description of the NMC global data assimilation and forecast system. Wea. and Forecasting, 4, 335-342.

44. Kanamitsu, M., J.C. Alpert, K.A. Campana, P.M. Caplan, D.G. Deaven, M. Iredell, B. Katz, H.-L. Pan, J. Sela, and G.H. White, 1991: Recent changes implemented into the global forecast system at NMC. Wea. and Forecasting, 6, 425-435.

45. Kiehl, J.T., J. J. Hack, G. B. Bonan, B. A. Boville, D. L. Williamson, and P. J. Rasch, 1998: The national center for atmospheric research community climate model CCM3. J. Climate, 11,1131-1149.

46. Kim, Y-J and A. Arakawa, 1995: Improvement of orographic gravity wave parameterization using a mesoscale gravity wave model. J. Atmos. Sci. 52, 11, 1875-1902.

47. Koepke, P., M. Hess, I. Schult, and E.P. Shettle, 1997: Global aerosol data set. MPI Meteorologie Hamburg Report No. 243, 44 pp.

48. Lacis, A.A., and J. E. Hansen, 1974: A parameterization for the absorption of solar radiation in the Earth's atmosphere. J. Atmos. Sci., 31, 118-133.

49. Leith, C.E., 1971: Atmospheric predictability and two-dimensional turbulence. J. Atmos. Sci., 28, 145-161.

50. Lindzen, R.S., 1981: Turbulence and stress due to gravity wave and tidal breakdown. J. Geophys. Res., 86, 9707-9714.

51. Matthews, E., 1985: "Atlas of Archived Vegetation, Land Use, and Seasonal Albedo Data Sets.", NASA Technical Memorandum 86199, Goddard Institute for Space Studies, New York.

52. Mitchell, K. E. and D. C. Hahn, 1989: Development of a cloud forecast scheme for the GL baseline global spectral model. GL-TR-89-0343, Geophysics Laboratory, Hanscom AFB, MA.

53. Mlawer, E.J., S.J. Taubman, P.D. Brown, M.J. Iacono, and S.A. Clough, 1997: Radiative transfer for inhomogeneous atmospheres: RRTM, a validated correlated-k model for the longwave. J. Geophys. Res., 102, 16663-16682.

54. Miyakoda, K., and J. Sirutis, 1986: Manual of the E-physics. [Available from Geophysical Fluid Dynamics Laboratory, Princeton University, P.O. Box 308, Princeton, NJ 08542.]

55. NMC Development Division, 1988: Documentation of the research version of the NMC Medium-Range Forecasting Model. NMC Development Division, Camp Springs, MD, 504 pp.

56. Pan, H-L. and L. Mahrt, 1987: Interaction between soil hydrology and boundary layer developments. Boundary Layer Meteor., 38, 185-202.

57. Pan, H.-L. and W.-S. Wu, 1995: Implementing a Mass Flux Convection Parameterization Package for the NMC Medium-Range Forecast Model. NMC Office Note, No. 409, 40pp. [Available from NCEP, 5200 Auth Road, Washington, DC 20233]

58. Pierrehumbert, R.T., 1987: An essay on the parameterization of orographic wave drag. Observation, Theory, and Modelling of Orographic Effects, Vol. 1, Dec. 1986, European Centre for Medium Range Weather Forecasts, Reading, UK, 251-282.

59. Ramsay, B.H., 1998: The interactive multisensor snow and ice mapping system. Hydrol. Process. 12, 1537-1546.

60. Reynolds, R. W. and T. M. Smith, 1994: Improved global sea surface temperature analyses. J. Climate, 7, 929-948.

61. Roberts, R.E., J.A. Selby, and L.M. Biberman, 1976: Infrared continuum absorption by atmospheric water vapor in the 8-12 micron window. Appl. Optics., 15, 2085-2090.

62. Rodgers, C.D., 1968: Some extension and applications of the new random model for molecular band transmission. Quart. J. Roy. Meteor. Soc., 94, 99-102.

63. Schwarzkopf, M.D., and S.B. Fels, 1985: Improvements to the algorithm for computing CO2 transmissivities and cooling rates. J. Geophys. Res., 90, 10541-10550.

64. Schwarzkopf, M.D., and S.B. Fels, 1991: The simplified exchange method revisited: An accurate, rapid method for computation of infrared cooling rates and fluxes. J. Geophys. Res., 96, 9075-9096.

65. Sela, J., 1980: Spectral modeling at the National Meteorological Center, Mon. Wea. Rev., 108, 1279-1292.

66. Slingo, A., 1989: A GCM parameterization for the shortwave radiative properties pf water clouds. J. Atmos. Sci.,46, 1419-1427.

67. Slingo, J.M., 1987: The development and verification of a cloud prediction model for the ECMWF model. Quart. J. Roy. Meteor. Soc., 113, 899-927.

68. Slingo, A., 1989: A GCM parameterization for the shortwave radiative properties pf water clouds. J. Atmos. Sci.,46, 1419-1427.

69. Stephens, G. L., 1984: The parameterization of radiation for numerical weather prediction and climate models. Mon.Wea. Rew., 112, 826-867.

70. Staylor, W. F. and A. C. Wilbur, 1990: Global surface albedoes estimated from ERBE data. Preprints of the Seventh Conference on Atmospheric Radiation, San Francisco CA, American Meteorological Society, 231-236.

71. Sundqvist, H., E. Berge, and J. E. Kristjansson, 1989: Condensation and cloud studies with mesoscale numerical weather prediction model. Mon. Wea. Rev., 117, 1641- 1757.

72. Tiedtke, M., 1983: The sensitivity of the time-mean large-scale flow to cumulus convection in the ECMWF model. ECMWF Workshop on Convection in Large-Scale Models, 28 November-1 December 1983, Reading, England, pp. 297-316. \

73. Troen, I. and L. Mahrt, 1986: A simple model of the atmospheric boundary layer; Sensitivity to surface evaporation. Bound.-Layer Meteor., 37, 129-148

74. Xu, K. M., and D. A. Randall, 1996: A semiempirical cloudiness parameterization for use in climate models. J. Atmos. Sci., 53, 3084-3102.

75. Zeng, X., M. Zhao, and R.E. Dickinson, 1998: Intercomparison of bulk aerodynamical algorithms for the computation of sea surface fluxes using TOGA COARE and TAO data. J. Climate, 11, 2628-2644.

76. Zhao, Q. Y., and F. H. Carr, 1997: A prognostic cloud scheme for operational NWP models. Mon. Wea. Rev., 125,1931-1953.

77. *McClain, C.R., R.S. Fraser, J.T. McLean, M. Darzi, J.K. Firestone, F.S. Patt, B.D. Schieber, R.H. Woodward, E-n. Yeh, S. Mattoo, S.F. Biggar, P.N. Slater,

K.J. Thome, A.W. Holmes, R.A. Barnes, and K.J. Voss, 1994: Case Studies for SeaWiFS Calibration and Validation, Part 2. NASA Tech. Memo. 104566, Vol. 19, S.B. Hooker, E.R. Firestone, and J.G. Acker, Eds., NASA Goddard Space Flight Center, Greenbelt, Maryland, 73 pp.

78. M. Wang, The Raleigh lookup tables for the SeaWiFS data processing: accounting for the effects of ocean surface roughness, Int. J. Remote Sensing, 2002, Vol 23, No. 13, 2693-2702.

79. M. Wang and W. Shi, Cloud Masking for Ocean Color Data Processing in the Coastal Regions, IEEE Transactions on Geoscience and Remote Sensing, Vol 44, No.11, November 2006, 3196-3205.

80. H.R. Gordon and M. Wang, Retrieval of water-leaving radiance and aerosol optical thickness over the ocean with SeaWiFS: A preliminary algorithm, Applied Optics, Vol. 33, No. 3, pp 443-452, Jan 1994.

81. M. Wang and Sean W. Bailey, Correction of sun glint contamination on the SeaWiFS ocean and atmosphere products, Applied Optics, Vol. 40, No. 27, pp 4790-4798, Sep 2001.